Do Dairy Digesters Reduce Methane Emissions? Evidence from Airborne Remote Sensing

Lauren Beatty [1], David McLaughlin [1], Wendong Zhang [2], Jasmin Wehner [2], and Mei Mei Collins[3]

[1]Environmental Defense Fund
[2]Cornell University
[3]University of California, Berkeley

October 27, 2026

Abstract

Globally, livestock, primarily beef and dairy cattle, account for roughly one-third of anthropogenic methane emissions. Despite this, empirical evidence on actual emissions at the dairy farm level remains scarce and largely limited to case studies. Accordingly, agri-environmental subsidies rely primarily on engineering projections. This paper uses aerial point-source remote sensing to measure the effect of an agri-environmental subsidy on methane emissions. We match Carbon Mapper airborne methane retrievals to 2,115 California dairy farms over 2016–2025, link them to the administrative records of the state's dairy anaerobic digester cost-share program, and estimate a staggered difference-in-differences regression that accounts for variation in treatment timing, using farms that have not yet installed a digester as controls. We find that digester installations reduce measured emissions by 113.22 kilograms per hour (95 percent confidence interval: 45.40 to 181.05), about 992 metric tons of methane per farm-year, and lowers the share of overpasses with a detectable plume by 46.6 percentage points. We estimate that realized reductions are 1.59 times the mean projection at the program level. We also calculate that public spending per realized ton of methane is $162, well below the $1,778 social cost of a combusted ton.

Keywords: Methane; Remote sensing; Environmental measurement; Anaerobic digesters; Dairy; Agricultural subsidies; Policy evaluation; Additionality; Greenhouse gas; Climate change

JEL codes: Q12, Q52, Q53, Q58, H23, C81, Q16

Acknowledgments: This work was supported by gifts to Environmental Defense Fund and Cornell Atkinson Center for Sustainability from the David and Patricia Atkinson Foundation. We thank participants from the 2026 AAEA Annual Meeting and the 2026 Anaerobic Digestion on the Farm conference for helpful comments.

Conflicts of interest: The authors declare no ties to the agricultural industry and no other conflicts of interest. This paper has not been accepted for publication and is not scheduled to

be published before the conference date.

1 Introduction

Governments pursue emissions mitigation often by subsidizing abatement investments. In contrast to an emissions tax, which conditions incentives on realized emissions, a subsidy pays for expected abatement before that abatement occurs. Credited abatement can exceed abatement in cases when the technology or practice delivers fewer reductions than assumed or in cases when the subsidy is awarded to actors that would have adopted the technology or practice irrespective of governmental financial support. Concerns about the effectiveness of these financial incentives have grown. Federal cost-share programs, such as the Rural Energy for America Program (REAP), have recently been suspended, and researchers and environmental groups question the net emissions effect of capital-intensive abatement investments in the agricultural sector (Friends of the Earth, 2026; Magesh et al., 2025).

We address these concerns by measuring the methane emission reductions from heavily subsidized anaerobic digester adoption by Californian dairy farms. Digesters decompose manure in oxygen-free tanks or covered lagoons and capture the resulting methane as biogas. Farms can burn this biogas to generate power on site, upgrade it to renewable natural gas for pipeline injection, or flare it, which converts the methane to CO_2 (U.S. Environmental Protection Agency, 2026). Since manure methane is an externality, dairy farmers have little private reason to invest in digesters, so emission reductions depend on outside incentives. California is a particularly relevant setting because of the scale of these incentives. Over the past decade, the Dairy Digester Research and Development Program (DDRDP) has provided $242.3 million toward 150 digesters, covering on average 30 percent of installation costs. According to the program report, these digesters reduce methane emissions from manure management in California by roughly one quarter and total greenhouse gas emissions from the state's agricultural sector by 8.4 percent (California Department of Food and Agriculture, 2025).

Whether these reductions are realized, however, depends on how digesters perform in reality. A growing body of literature documents fugitive emissions from digesters, including leaks from pressurized equipment, unburnt methane from engines and flares, and emissions from reactor feeding systems (Baldé et al., 2022; Debruyn et al., 2020). Large public expenditures combined with evidence of fugitive emissions have fueled a public debate about whether digesters effectively reduce emissions. This debate demonstrates the need for a comprehensive assessment of the net effect of digester installations on methane emissions.

We provide a comprehensive estimate of the effect of digester installation on methane emissions using aerial remote sensing data, which are increasingly used in agricultural and environmental economics (Aker et al., 2026; Wuepper et al., 2025). Carbon Mapper's airborne imaging spectrometers repeatedly overfly California's dairy regions and record point-source methane plumes, each with an estimated emission rate. We match these measurements to 2,115 dairy farms from the California Dairy & Livestock Database from 2016 to 2025. We study the effect of digesters on emissions by using the measured emission rate in kilograms per hour, and

persistence, defined as the share of overpasses at which a plume is detected at all. To estimate the effect of installation on these outcomes, we apply the staggered difference-in-differences estimator of Callaway and Sant'Anna (2021). Identification comes from comparing the change in measured emissions at a farm around its own installation date with the contemporaneous change at farms that have not yet installed a digester. Finally, we compare our estimated reductions with the reductions projected for DDRDP projects (California Department of Food and Agriculture, 2025) and relate them to farm-level installation costs from the program's administrative records.

We show, first, that digester installation reduces measured emissions by 113.22 kg/hr, with a 95 percent confidence interval of 45.40 to 181.05 kg/hr, and the estimate moves only to 108.56 kg/hr when every non-detect is entered at the detection limit instead of at zero. Censoring at the airborne detection limit is too small a correction to account for the effect. Persistence falls by 46.6 percentage points, so most of the reduction operates by shrinking detectable plumes to zero or non-detectable.

Second, we find that the realized reduction is larger than the reduction projected for DDRDP awards, though it is not estimated precisely enough to establish over-delivery. The mean DDRDP project projects 71.1 kg CH_4/hr and the median projects 65.9kg/hr, against a realized 113.2 kg/hr.[1] The point estimate is 1.59 times the mean projection, but the confidence interval includes reductions as small as 45.40 kg/hr, smaller than the mean projection, so we cannot rule out that digesters deliver less than the engineering projections. What we can say is that the wedge documented in the energy efficiency setting, where realized savings fall well short of projected savings, does not appear with the same sign here.

Third, we show that the public cost per ton of realized abatement is below the cost per ton the projections imply, and both are below the social cost of the methane averted. Dividing mean DDRDP cost share by realized ten-year abatement gives $162 per ton of methane, against $258 per ton at the projected reduction; including the private share of project costs raises the realized figure to $543 per ton. The social cost of a ton of methane is $2,494 if it vents, and $1,778 once the CO_2 produced by burning it is netted out (U.S. Environmental Protection Agency, 2023).[2]

Closest to our paper is Valdez et al. (2026), who use the same Carbon Mapper aircraft data to compare emissions at 98 California dairies before, during, and after digester installation. They document a temporary increase during construction and a net decline in mean point-source emissions from 91 to 68 kg CH_4 per hour. Their design compares each farm with itself across installation phases. We add a control group by comparing treated farms with farms that have not yet installed a digester. In companion work, Ai et al. (2026) show that column-averaged satellite methane locates concentrated livestock activity across the globe but cannot evaluate individual farms; we work inside that detection envelope with facility-scale retrievals

[1] The projections are reported in MT CO_2e over a ten-year horizon; converting them to methane tons uses a 100-year global warming potential of 28. At 113.2 kg/hr held continuously, a treated farm averts about 992 metric tons of methane per year.

[2] These are gross figures because we do not account for digester revenue yet. Digester operators also earn the wholesale value of the gas, LCFS credits, and RINs (Renewable Identification Numbers). Counting them would raise the public cost per ton, so the figures presented in this paper are a lower bound.

to measure what a subsidy actually changes. Our paper also relates to studies that compare ex-ante projections of policy benefits with ex-post outcomes. Our paper also relates to studies that compare ex-ante projections of policy benefits with ex-post outcomes. Fowlie et al. (2018) run this comparison for the Weatherization Assistance Program, and Christensen et al. (2023) and Burlig et al. (2020) run it for residential and school energy efficiency retrofits. These papers compare engineering models of energy savings with realized consumption. We compare engineering projections of methane abatement with realized emissions measured from the air.

Recent work has developed structural methods to infer unobserved firm-level abatement from production data under market-based carbon pricing (Butters et al., 2026). Capital-subsidy programs raise a different question because they fund a specific abatement technology, the question is whether that technology delivers the reduction it was assumed to deliver. To our knowledge, our paper provides the first quasi-experimental estimate of the effect of digesters on farm-level methane emissions, and the first comparison of realized reductions with the projections on which the subsidies were awarded. We also demonstrate how aerial point-source remote sensing can measure farm-level methane emissions at the scale and frequency that evaluating an agri-environmental program requires. In doing so, we extend the growing use of remote sensing as a measurement tool in agricultural and environmental economics (Aker et al., 2026; Henningsen et al., 2025; Wuepper et al., 2025).

The remainder of the paper proceeds as follows. Section 2 provides institutional background on manure management, financial incentives, and emission measurement for anaerobic digesters in California. Section 3 sets out the estimator and the censoring bracket. Section 4 describes the airborne point-source data and the administrative cost-share records. Section 5 reports the event-study results and converts them into tons abated and dollars per ton. Section 6 discusses what the detection measures imply for interpretation and for the additionality of the subsidy, and Section 7 concludes.

2 Background

2.1 Manure Management in California's Dairy Sector

Livestock production in the United States increasingly clusters in concentrated animal feeding operations (CAFOs), large facilities that raise many animals on small land areas to achieve greater efficiency and lower cost. CAFOs also concentrate the pollution externalities of animal agriculture, primarily through manure (Chen et al., 2025). Because improperly stored or over-applied manure can spill or run off into nearby waterways and degrade water quality, the Clean Water Act regulates CAFOs as point sources and requires them to maintain nutrient management plans (Del Rossi et al., 2023).

Manure methane can be considered as an externality of milk production. There are no direct cost when methane escapes from manure storage. A herd of several thousand cows often produces more manure than nearby cropland can absorb, so dairies flush their barns with water and store the resulting slurry in large anaerobic lagoons. The lagoons hold liquid manure in an oxygen-free environment for months at a time and create therefore ideal conditions for

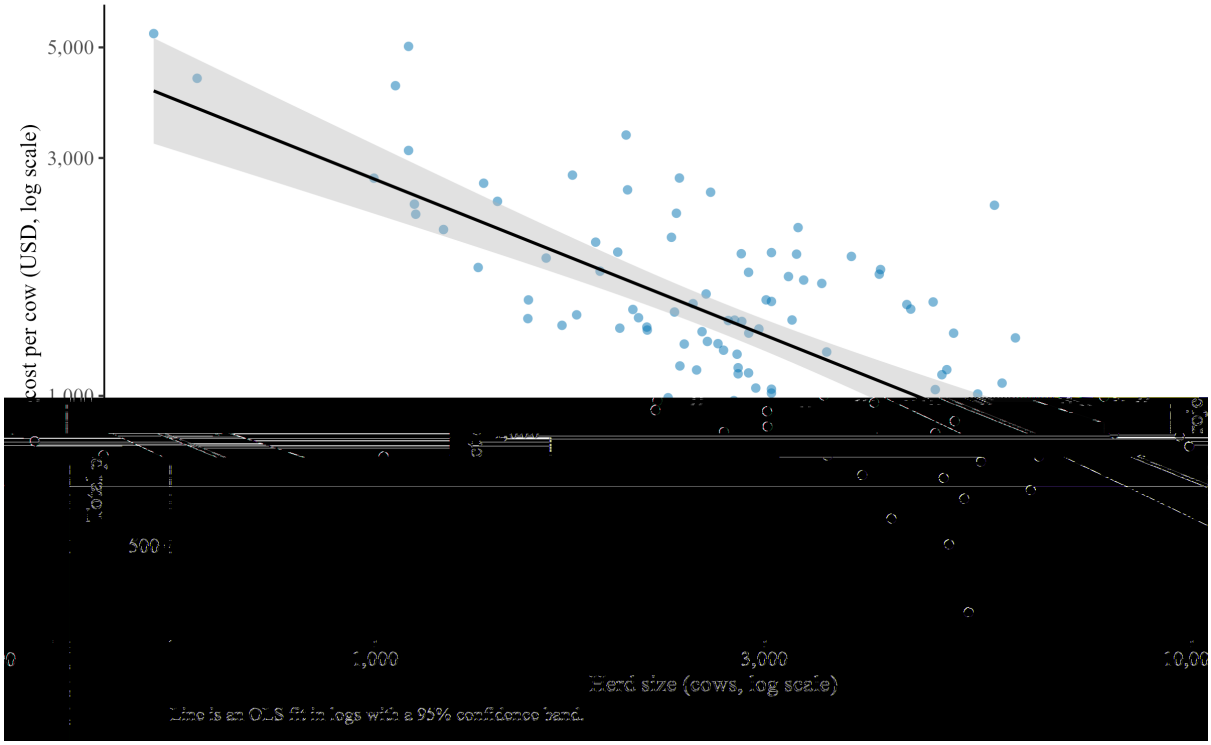


Figure 1: Digester cost per cow against herd size.

methane-producing microbes. The IPCC assigns uncovered anaerobic lagoons in warm climates a methane conversion factor of roughly 76 percent, among the highest of any manure management system (Intergovernmental Panel on Climate Change , IPCC, Table 10.17).

California supports manure-management practices aimed at reducing methane emissions through multiple cost-share programs. Matching documented cost-share projects to herd-size data, we find that across 68 such digester projects, on farms with 2,852 cows on average, digesters deliver the largest per-cow abatement (0.0237 $MTCO_2e$ per cow per year). This abatement also draws the largest public investment: anaerobic digesters receive $1,990 in cost share per cow, compared with $245 for composting and under $48 for the drying and storage practices. Anaerobic digesters seem to be the manure-management practice with both the largest emission reductions and the largest public financial support (California Department of Food and Agriculture, 2026, 2025). Figure 1 plots total project cost per cow against herd size across digester projects, illustrating economies of scale related to the high fixed cost capital investment.

2.2 Incentives for Anaerobic Digester Installations

The most prominent incentives for new digester installation are cost-share programs, which reduce the reported fixed installation costs that range from USD 1,779,865 to USD 14,298,076 across the Dairy Digester Research and Development Program (DDRDP) projects. DDRDP has provided up to 50 percent cost share for digesters with any biogas end use[3] built in California since 2015. Across all years, the program has provided $242.3 million for 150 dairy digesters. The annual budget was $11 million in 2014–2015, peaked in 2018 at $74.32 million, and stands

[3]electricity, hydrogen, renewable natural gas

at $7 million for 2025–26. Prospective digester operators submit their applications using a calculation tool provided by the California Air Resources Board (CARB), and applications are reviewed and scored on six weighted criteria spanning financial and environmental performance, with estimated greenhouse gas emissions reduction and environmental performance together accounting for half of the total score. Matching funds are desired but not mandatory, and the program has held a series of outreach and application workshops to encourage uptake (California Department of Food and Agriculture, 2025). Importantly, the DDRDP does not fund upgrades of existing digesters and does not allow a herd size increase from the date of application through the end of the project term. The herd-size condition matters for interpreting post-adoption herd trajectories at treated farms.

A second grant scheme is the Biomethane Monetary Incentive Program, which has provided cost share payments for RNG-producing digesters built in California since 2015. It initially covered up to 50 percent of interconnection costs, up to $1.5 million per project; the cap doubled to $3 million per project in 2016, and a cluster of at least three dairies that successfully interconnects with the natural-gas pipeline system and operates by December 31, 2026 can instead receive $5 million per project (California State Legislature, 2026).

California's Low Carbon Fuel Standard (LCFS) is a market-based crediting program designed to decarbonize the state's transportation sector. The program rates fuels by carbon intensity (CI): fuels scoring below an annually declining benchmark generate credits in proportion to how far below the benchmark they fall, while fuels above it generate deficits, and producers of low-CI fuels sell credits to suppliers of higher-CI fossil fuels. Since 2017, dairy biogas has qualified for a low CI score, so dairy farmers can earn income by selling credits. Because the LCFS operates on a book-and-claim basis, every dairy farmer who produces renewable natural gas is eligible. The volatility of California's LCFS credit prices, however, makes a digester's financial viability dependent on favorable credit-market conditions (California State Legislature, 2016; Lazenby, 2024).

Once manure methane is captured, the LCFS credits it according to the fuel it becomes. The dominant certified pathway upgrades biogas to pipeline-quality biomethane dispensed as compressed natural gas in heavy-duty trucks; a second set of pathways burns biogas in on-site engines to generate electricity supplied to electric-vehicle charging, and the regulation also provides for fuel-cell electricity and biomethane-derived hydrogen (California Air Resources Board, 2025; Seber et al., 2024). Because CARB nets the avoided lagoon methane against the fuel's processing and combustion emissions, certified carbon intensities are steeply negative. First, the approved dairy biomethane pathways range from -151 to -533 gCO_2e per megajoule and average roughly -313. Second, the certified digester-electricity pathways range from -593 to -758 gCO_2e per megajoule and average roughly -643. Third, and finally, the fuel-cell electricity carries a flat lookup value of -300; and dairy biomethane reformed to hydrogen averages about -201 (California Air Resources Board, 2024, 2025; Seber et al., 2024).

These values reflect the program's crediting convention as much as the fuels themselves. CARB certifies dairy pathways against a baseline of continued anaerobic lagoon storage, the prevailing manure-management practice at credited farms, so each megajoule of fuel carries

a credit for the methane it embodies, roughly 20 grams of CH_4, or some -500 gCO_2e at a global warming potential of 25 that is assumed otherwise to have been emitted (California Air Resources Board, 2025). The LCFS uses the fuel's carbon intensity as the vehicle for crediting avoided methane, and CARB's own analysis reports an average dairy biomethane CI of approximately 36 gCO_2e per megajoule when the avoided-methane credit is excluded (California Air Resources Board, 2024). The same convention explains the dispersion across pathways: a similar credit is spread over different energy denominators, so pathways with lower conversion efficiency show more negative per-megajoule values. The size of realized abatement therefore depends on both the counterfactual manure management and on how much captured methane escapes before combustion. These quantities the certification process projects from engineering parameters rather than observing them. This paper attempts to estimate these quantities directly.

Electricity-producing digesters can also participate in the Bioenergy Market Adjusting Tariff (BioMAT) program, which since 2016 has paid small-scale bioenergy generators (up to 5 MW, within a 90 MW program cap) a bi-monthly-updated fixed price for power—$188 per MWh for dairy projects as of December 2025 (California Public Utilities Commission, 2026).

The successful installation and operation of an anaerobic digester therefore depends on a combination of upfront cost share and ongoing returns from volatile credit markets. A recent survey among digester operators found that cost share programs are the single most essential decision factor for current and new digester installations (Wehner et al., 2026). Given the scale of abatement and public support established in the previous two subsections, we focus in this paper on manure stored and combusted via anaerobic digesters.

2.3 Emissions Measurements Related to Anaerobic Digesters

The literature on field measurements of methane-reduction potential of anaerobic digesters is mixed. Studies differ in how they measure methane as well as in their geographic focus. Some studies find substantial declines in emissions after digester installation, whereas others report increases in total methane due to fugitive leaks from the digester system. The net climate impact of digesters therefore remains site- and context-dependent and empirically uncertain.

Measurement strategies range from the ground to the air. Mobile-laboratory campaigns sample ambient methane concentrations around a single site over several days and test for distributional shifts (Rodriguez et al., 2025). Multi-instrument site studies compare facility-level flux estimates across techniques and against EPA bottom-up inventory methods, as Arndt et al. (2018) do for two California dairies with different manure-storage systems. Airborne shortwave-infrared imaging spectrometers, such as those Carbon Mapper operates, extend measurement from single sites to point-source inventories spanning many farms; Valdez et al. (2026) use such an inventory to track California dairies across digester installation phases. The introduction describes how our design builds on theirs; here we note only that the airborne approach trades site-level detail for repeated coverage of many farms, which is what a panel research design requires.

Combustion in any of the pathways above converts the captured methane to CO_2. Venting does the same, only slower: methane emitted to the atmosphere is oxidized by hydroxyl radicals to CO_2 over a perturbation lifetime of roughly twelve years (Forster et al., 2021). Because the carbon in manure methane was recently fixed by photosynthesis, the resulting CO_2 is climate-neutral under either outcome. Capture avoids a decade during which the same carbon resides in the atmosphere as methane, with roughly 27 times the hundred-year warming impact (Forster et al., 2021). The U.S. Environmental Protection Agency (2023) estimates that the social cost of methane is \$2,494 per metric ton (2025 dollars) while the social cost of CO_2 is \$261 per metric ton. Calbry-Muzyka et al. (2022) report that measured cow biogas was 54.9% methane and 39% CO_2. This gas, if not combusted, would yield \$955 in social cost damages per metric ton of biogas: \$793 from methane and \$162 from the co-released CO_2. Combustion shrinks the damage to \$390, a reduction of roughly 59%.

3 Empirical Strategy

We estimate the effect of digester installation on farm-level methane emissions measured by Carbon Mapper's airborne retrievals using a staggered difference-in-differences design that compares farms after installation with farms that have not yet installed a digester.

There are strong reasons to expect treatment effects in this setting to vary both across adoption cohorts and over time since adoption. Cohorts adopt under different incentives—grant availability, the anticipation of prevailing fuel-credit prices, and regulatory pressure all shift over the sample period—and differ systematically in herd size and manure-management practices. Within a cohort, effects may also evolve with time since installation as digesters ramp up, are maintained with varying diligence, or degrade. This heterogeneity is consequential for estimator choice. Conventional two-way fixed-effects estimators can produce difficult-to-interpret or biased estimates when treatment effects vary across cohorts or over time: already-treated farms serve as implicit controls for newly treated farms, and the resulting estimator may assign negative weights to some underlying treatment effects (de Chaisemartin and D'Haultfœuille, 2020; Goodman-Bacon, 2021; Sun and Abraham, 2021; Borusyak et al., 2024). We therefore follow Callaway and Sant'Anna (2021), estimating treatment effects separately by adoption cohort and calendar period using only farms that remain untreated in the relevant comparison period.

Choice of Estimator Several estimators address these shortcomings of two-way fixed effects (de Chaisemartin and D'Haultfœuille, 2020; Sun and Abraham, 2021; Wooldridge, 2025; Borusyak et al., 2024); Baker et al. (2026) provide a synthesis of these designs and practical guidance on choosing among them. Three features of our setting favor the Callaway and Sant'Anna (2021) framework. First, digester adoption is strongly related to herd size, so parallel trends is plausible only conditional on covariates; the doubly robust estimator of Sant'Anna and Zhao (2020), on which the framework builds, accommodates covariate-conditional trends without requiring a correctly specified outcome model. Second, permitting, financing, and construction lags create scope for anticipatory changes in manure management before the recorded operating

date, and the framework incorporates a user-specified anticipation window that adjusts both the reference period and the eligible comparison set. Third, the group-time building blocks make the comparison group explicit, allowing us to report specifications using never-treated and not-yet-treated controls that invoke different, clearly stated parallel-trends assumptions. By contrast, imputation-style estimators (Borusyak et al., 2024) gain precision by imposing parallel trends across all pre-treatment periods, an assumption we view as unattractive given the noisiness of remote-sensing outcomes.

3.1 Estimating Framework

Let Y_{it} denote the methane outcome for farm i in period t. We examine two outcomes: (1) mean measured methane emissions, expressed in kilograms per hour, and (2) emissions persistence, defined as the proportion of valid remote-sensing overpasses in which a methane plume is detected.

Let G_i denote the first period in which farm i has an operational digester according to the administrative records. We set $G_i = \infty$ for farms that are not observed adopting a digester during the sample period. Let $Y_{it}(g)$ denote the potential outcome in period t if farm i first adopts a digester in period g, and let $Y_{it}(\infty)$ denote the potential outcome if the farm remains untreated. For each adoption cohort g and post-treatment period $t \geq g$, the group-time average treatment effect on the treated is

$$ATT(g,t) = \mathbb{E}\left[Y_{it}(g) - Y_{it}(\infty) \mid G_i = g\right]. \tag{1}$$

Thus, $ATT(g,t)$ measures the average effect in period t among farms whose digesters first became operational in period g. Defining effects at the cohort-period level allows both the initial effect of adoption and its subsequent evolution to differ across cohorts, matching the sources of heterogeneity described above.

We estimate each $ATT(g,t)$ using the doubly robust difference-in-differences estimator of Sant'Anna and Zhao (2020), as incorporated into the staggered-adoption framework of Callaway and Sant'Anna (2021). The estimator combines an outcome-regression model with inverse-probability weighting based on the estimated propensity to belong to a given adoption cohort. Subject to the identifying assumptions below, the estimator remains consistent if either the outcome-regression model or the propensity-score model is correctly specified.

Because some adoption cohorts contain few farms, individual group-time estimates can be imprecise. Our inferential targets are therefore aggregated parameters rather than the underlying $ATT(g,t)$. We report two principal summaries. First, we calculate an overall ATT by averaging post-treatment effects within each cohort and then averaging across cohorts using weights proportional to cohort size. This weighting gives greater influence to cohorts containing more treated farms without using already-treated farms as controls. Second, we estimate dynamic treatment effects by event time:

$$ATT(e) = \sum_{g:g+e\leq T} \omega_g(e)\, ATT(g, g+e), \qquad e \geq 0, \tag{2}$$

where $e = t - g$ is the number of periods relative to digester adoption and $\omega_g(e)$ denotes the cohort-size weight among cohorts observed at event time e. We also construct analogous pre-treatment placebo estimates for $e < 0$. In the baseline event-study specification, we use the final pre-treatment period, $e = -1$, as the universal reference period. Consequently, each event-study coefficient represents the difference relative to the period immediately preceding adoption rather than a period-over-period change based on a varying reference period.

3.2 Identification

Identification of the group-time treatment effects requires no anticipation, conditional parallel trends, and sufficient overlap between treated and comparison farms.

Assumption 1: No anticipation. Our baseline specification assumes that farms do not change their methane outcomes in response to future digester adoption before the digester becomes operational:

$$Y_{it}(g) = Y_{it}(\infty) \qquad \text{for all } t < g. \tag{3}$$

This assumption warrants particular attention in our setting because obtaining permits, financing, and constructing a digester can take considerable time. Farms might alter manure-storage or management practices during this period, before the recorded operating date. We therefore supplement the baseline specification with estimates that allow for $\delta \in \{1, 2\}$ periods of anticipation. Under an anticipation window of length δ, the restriction becomes

$$Y_{it}(g) = Y_{it}(\infty) \qquad \text{for all } t < g - \delta, \tag{4}$$

and the last period assumed to be unaffected by treatment is $g - \delta - 1$. These specifications allow outcomes to begin responding as much as one or two periods before the recorded adoption date.

Assumption 2: Conditional parallel trends. Let $b_g(\delta) = g - \delta - 1$ denote the last uncontaminated pre-treatment period for cohort g, and let $\mathcal{C}_{g,t}(\delta)$ denote the set of farms eligible to serve as controls for that cohort and period. Conditional parallel trends requires that, absent digester adoption, farms in cohort g and eligible control farms would have experienced the same average change in methane outcomes:

$$\begin{aligned} &\mathbb{E}\left[Y_{it}(\infty) - Y_{i,b_g(\delta)}(\infty) \mid G_i = g, X_i = x\right] \\ &\quad = \mathbb{E}\left[Y_{it}(\infty) - Y_{i,b_g(\delta)}(\infty) \mid i \in \mathcal{C}_{g,t}(\delta), X_i = x\right] \end{aligned} \tag{5}$$

for all relevant cohorts, post-treatment periods, and covariate values in the common support. In the baseline specification, X_i includes pre-treatment herd size. Because herd size is strongly associated with both digester adoption and potential methane emissions, conditioning on it improves the comparability of treated and untreated farms. All covariates are measured before treatment so that they cannot themselves be affected by digester adoption.

For the not-yet-treated comparison group,

$$\mathcal{C}_{g,t}^{\mathrm{NYT}}(\delta) = \{i : G_i > t + \delta\}\,. \tag{6}$$

Under the baseline assumption of no anticipation, this set consists of farms that have not adopted a digester by period t, including later adopters and farms that remain untreated throughout the sample. When anticipation is permitted, we additionally exclude farms that are sufficiently close to their own adoption date that their outcomes may already be responding.

For the never-treated comparison group,

$$\mathcal{C}_{g,t}^{\mathrm{NT}} = \{i : G_i = \infty\}\,. \tag{7}$$

The two control groups therefore invoke different versions of the parallel-trends assumption. The not-yet-treated specification compares adopters with farms that may eventually adopt and are therefore potentially drawn from a more similar selection pool. The never-treated specification instead requires that adopters would have followed the same untreated trajectory as farms that never adopt during the sample. Restricting the controls to never-adopters eliminates the possibility that a control farm is already adjusting in anticipation of its own adoption, but it does not eliminate possible anticipation by the treated cohort.

Parallel trends is not invariant to transformations of the outcome, so the scale on which Equation (5) is imposed is a substantive modeling choice (Roth and Sant'Anna, 2023). We state the assumption in levels—kilograms per hour for measured emissions and detection proportions for persistence—because these are the scales on which the physical process of methane capture operates and on which policy quantities such as abated tons are defined.

Assumption 3: Overlap. The doubly robust estimator also requires sufficient overlap in observed characteristics between each treated cohort and its eligible comparison group. In particular, conditional on X_i, farms must have a positive probability of belonging to both the treated cohort and the relevant control group. We examine the distribution of herd size across treatment cohorts and comparison farms to assess common support.

Assessing the identifying assumptions. We assess the plausibility of conditional parallel trends using the pre-treatment placebo coefficients from the dynamic specification. We present both the individual pre-treatment estimates and a joint test of the hypothesis that all pre-

treatment effects are zero. We also examine whether the conclusions are sensitive to allowing one or two periods of anticipation.

These diagnostics are informative but do not establish the identifying assumption. Pre-trend tests may have limited power, particularly when outcomes are noisy, and parallel trends in the post-treatment counterfactual are inherently unobservable (Roth, 2022; Roth et al., 2023). We therefore interpret a failure to reject the joint pre-trend hypothesis as supporting evidence rather than proof of parallel trends.

3.3 Specification Choices

We estimate specifications that vary in the construction of the Carbon Mapper outcomes, the definition of the comparison group, and the allowance for anticipatory responses.

Carbon Mapper data construction. We construct the Carbon Mapper farm-level panel in two ways:

- **Source-based approach.** We link each farm to the nearest identified Carbon Mapper methane source and use observations in which the remote-sensing instrument directly retrieves emissions from that source. This approach provides a consistent source definition over time and reduces the risk that measurements are attributed to different nearby emission points. Its principal limitation is that it produces a smaller and potentially selected sample, particularly for farms whose emissions are detected infrequently.
- **Footprint-based approach.** We construct an observation whenever a farm falls within the valid spatial footprint of a Carbon Mapper survey overpass, regardless of whether the farm is coded as an emitting source during that overpass. This approach allows valid non-detections to contribute to the persistence measure and substantially expands the number of farm-overpass observations. It may, however, exacerbate measurement error when a non-detection reflects wind, visibility, the instrument's detection threshold, or other observation conditions rather than the true absence of emissions.

The source-based approach emphasizes consistency in the identity of the measured emission point, whereas the footprint-based approach more fully uses information from overpasses in which the instrument had an opportunity to detect emissions. We report both to evaluate the sensitivity of the results to these alternative measurement constructions.

Comparison Groups. Our primary specification uses not-yet-treated farms as controls. At each (g, t) comparison, this excludes farms that have already installed digesters while retaining later adopters that remain untreated and outside any specified anticipation window. These later adopters may provide especially informative counterfactuals because they ultimately select into the same program or technology.

As a robustness specification, we use only farms that never install a digester during the sample period. This restriction avoids using farms that are approaching their own treatment dates, but it may reduce precision and comparability if never-adopters differ systematically from adopters

in farm scale, production technology, management, or other determinants of methane emissions. No anticipation by the treated cohort remains necessary under both definitions of the control group.

Anticipation Windows. The baseline specification sets $\delta = 0$, treating the period immediately before the recorded operating date as the reference period. We then re-estimate the model allowing outcomes to respond one or two periods before adoption. In these specifications, we shift the reference period to $g - \delta - 1$ and remove potentially anticipating farms from the not-yet-treated comparison group.

Two-way Fixed-effects Benchmark. For comparability with conventional empirical practice, we also report estimates from static and event-study regressions with farm and period fixed effects. We treat these estimates as descriptive benchmarks rather than as our preferred causal estimates because their interpretation can be affected by heterogeneous treatment effects and comparisons involving already-treated farms. Comparing the conventional and cohort-specific estimates helps reveal whether these issues are empirically important in our application.

3.4 Probability of Detection

A non-detect carries information about emissions only through the probability that the instrument would have seen a plume of a given size on that overpass. We write this probability of detection (POD) as $\pi(Q, U, h, e)$, where Q is the emission rate of the plume in kg/hr, U is wind speed, h is the aircraft's altitude above ground, and e is the distance from the source to the edge of the scene footprint. Q is the rate of the concentrated plume that the retrieval delineates.

We identify it instead from close repeat looks at the same livestock source. Carbon Mapper's aircraft often cover a source more than once in a day, because adjacent flight lines overlap and a second sortie often revisits the same area. Consider two airborne looks at a catalogued livestock source no more than 24 hours apart. The first look, the reference, detects a plume and quantifies its emission rate Q_r. The second look, the test, either detects a plume or misses it. A miss yields no emission rate, so we evaluate π at the reference rate Q_r and the test look's own conditions.

This approach treats Q_r as the true rate Q at the time of the test look. Q_r is a measurement and can differ from Q if emissions change between the two looks or if the reference look measures them with error. The approach therefore requires three conditions. First, the emission rate does not change between the two looks. Second, the two detection events are independent given the emission rate and look conditions. Third, Q_r measures the emission rate without error. Selecting pairs on detection at the reference look does not bias the estimate when the first two conditions hold, because π conditions on the emission rate.

The functional form follows the one Carbon Mapper fits to its controlled-release experiments (Carbon Mapper, personal communication), a Burr XII distribution function of a log-linear

index:

$$\pi(Q, U, h, e) = 1 - [1 + \exp(2\,z)]^{-1.5}, \qquad z = \alpha + \beta_Q \ln Q - \beta_U \ln U - \beta_H \ln h + \beta_E \min(e, 2), \quad (8)$$

with the two shape parameters fixed at Carbon Mapper's values. We estimate $(\alpha, \beta_Q, \beta_U, \beta_H, \beta_E)$ by maximum likelihood over test looks. Standard errors come from 500 bootstrap samples that resample sources, which accounts for the several pairs one sortie can produce at a single source.

Each covariate is defined for every look, whether or not it detects. Wind is the ERA5 10 m wind speed (Hersbach et al., 2020), interpolated to the time of the look. Carbon Mapper reports a wind speed only for detected plumes, so it cannot enter a model of detection. ERA5 is a coarse proxy for wind at the plume, and the measurement error attenuates β_U toward zero. The catalog does not record aircraft altitude, so we infer it from swath width, which equals $2h\tan(\phi/2)$ for an instrument with field of view ϕ; we take the width as the short side of the smallest rectangle enclosing each scene footprint. Edge distance runs from the catalogued source coordinate to the footprint boundary.

3.5 Inference

We conduct inference using the multiplier bootstrap proposed by Callaway and Sant'Anna (2021), clustering at the farm level to account for serial correlation in repeated observations of the same farm. The farm is also the level at which treatment is assigned, so clustering matches the design. For scalar summary parameters, including the overall ATT, we report 95 percent bootstrap confidence intervals.

For the dynamic event-study estimates, we report 95 percent simultaneous confidence bands constructed from the clustered multiplier bootstrap. Unlike pointwise confidence intervals, these bands control coverage jointly across the full event-time path. They are therefore particularly relevant when evaluating the collection of pre-treatment coefficients rather than testing each lead separately. We also report a joint test that all available pre-treatment placebo effects are equal to zero.

Because inference is clustered at the farm level, its reliability depends on the number of treated and untreated farms rather than the number of farm-period observations. As noted above, we do not emphasize inference on individual group-time effects, which can rest on few farms within a cohort, and instead focus on the aggregated parameters that pool information across cohorts.

All Callaway–Sant'Anna estimates are implemented in R using the `did` package. The event-study implementation uses a universal pre-treatment base period, with $e = -1$ normalized to zero in the baseline specification and $e = -\delta - 1$ used as the reference period in specifications allowing anticipation.

4 Data

4.1 Dairy Herd Size Data

We obtain dairy size, digester presence, and location information from the California Dairy & Livestock Database (CADD). The combined panel covers 2,115 farms over 2016 to 2025 and we display the average farm size per year and digester adoption status in Table 1 from 2016 to 2023 because of missing CADD herd size data for the last two years. Digester adoption and the Carbon Mapper observations continue through 2025. The table shows that average farm size declines over time for farms without a digester and rises for those with one. This pattern is consistent with economies of scale in digester installation but it cannot establish a causal relationship between herd size and digester adoption in either direction. Most digesters were installed in 2021 ($n = 39$) and 2022 ($n = 26$). Average farm size declined over the period, from 821 cows in 2016 to 638 in 2023, and the gap between adopters and non-adopters is wide throughout: in 2023 the average adopter milked 3,115 cows against 479 at farms without a digester. The latter number is in line with estimations which show that economic viability of digesters starts with 500 dairy cows (U.S. Environmental Protection Agency, 2018).

Table 1: Dairy farms and average herd size per year, by digester adoption status. Source: California Dairy & Livestock Database (CADD)

	Total		Non-adopters		Adopters	
Year	#farms	milk cows (avg.)	#farms	milk cows (avg.)	#farms	milk cows (avg.)
2016	2115	821	2096	801	19	2697
2017	2115	813	2094	790	21	2778
2018	2115	804	2089	773	26	2919
2019	2115	683	2081	643	34	3131
2020	2115	676	2070	623	45	3106
2021	2115	674	2031	566	84	3306
2022	2115	656	2005	515	110	3233
2023	2115	638	1987	479	128	3115

4.2 Carbon Mapper Observations

We use point-source detections of methane emissions events from Carbon Mapper. Carbon Mapper is a nonprofit emissions monitoring program that integrates data from multiple remote sensing platforms—aircraft and satellite—to detect, locate, and estimate methane and carbon dioxide emissions from industrial, waste, agricultural, and energy infrastructure. These instruments include, but are not limited to, Planet Labs' Tanager Satellites and NASA's Earth Surface Mineral Dust Investigation (EMIT) sensor (Carbon Mapper, 2026b). For this paper, we focus exclusively on the airborne observations. Measurements from aircraft have a far lower detection limit than satellite instruments, making them more suitable for accurately capturing methane emissions from dairy farms. The quantification skill of point-source methane remote sensing has been established in large controlled-release experiments: in a year-long single-blind test of 481 staged releases, purpose-built imaging spectrometers detected 92–100 percent of releases on

clear days and recovered release rates with regression slopes of 0.83–1.00 against the metered truth (Reuland et al., 2026).

Carbon Mapper provides data on:

- **Observation footprints:** The spatial area observed by the sensing instrument during a single overpass or acquisition. Footprints define the geographic coverage of each measurement and determine where detections were possible.
- **Emission sources:** Distinct geolocated facilities or infrastructure elements that have been observed emitting methane at least once during the study period. Sources represent persistent locations that may be associated with multiple plume detections over time.
- **Plume detections:** Individual observations of methane enhancements linked to a source. Plume records typically include an estimated emission rate (kg/hr), though sometimes only include a binary variable for whether a plume was observed or not.

4.3 Data Construction

We combine the dairy panel and Carbon Mapper records by spatially matching the dairies with methane data and construct the estimation data two ways. First, one can merge each dairy with the nearest Carbon Mapper "source" and then use the linked source data to determine when a source was observed and whether it was observed to be emitting or not. We refer to this data construction method as "source-based" for the remainder of this paper. Another method would be to join the spatial footprint of each remote sensing observation with our dairies, then use that spatial match to form the basis of whether there was an observation or not. We refer to this construction method as "footprint-based." The two constructions share exactly the same group of positive observations—overpasses at which the instrument records a plume—but differ in their negative observations. The "footprint-based" construction adds negative observations of two kinds. The first are farms *never* observed to be emitting, which are never linked to a "source" since they are not observed in the Carbon Mapper data. Second, there are "sources" that are within an observation footprint for a given observation, but not coded by Carbon Mapper as having an observation at that particular time and day. On average, these observations are cloudier, so we suspect that many of these rows are being filtered out due to poor observation quality.

4.4 Summary Statistics

Under either data construction, most observations are non-detects. Of the 4,649 airborne looks in the source-based sample, 80 percent record no plume; of the 9,290 looks in the footprint-based sample, 90 percent do. Figure 2 plots the distribution of measured emission rates, with the non-detects collected in a single bar to the left of the axis and split by the construction they belong to. Of these, 3,712 are source-based zeros, overpasses that Carbon Mapper coded as observations of the farm's source at which no plume was found, and a further 4,641 enter only under the footprint-based construction. The positive bars are common to the two constructions, so the split bar is the entire difference between them.

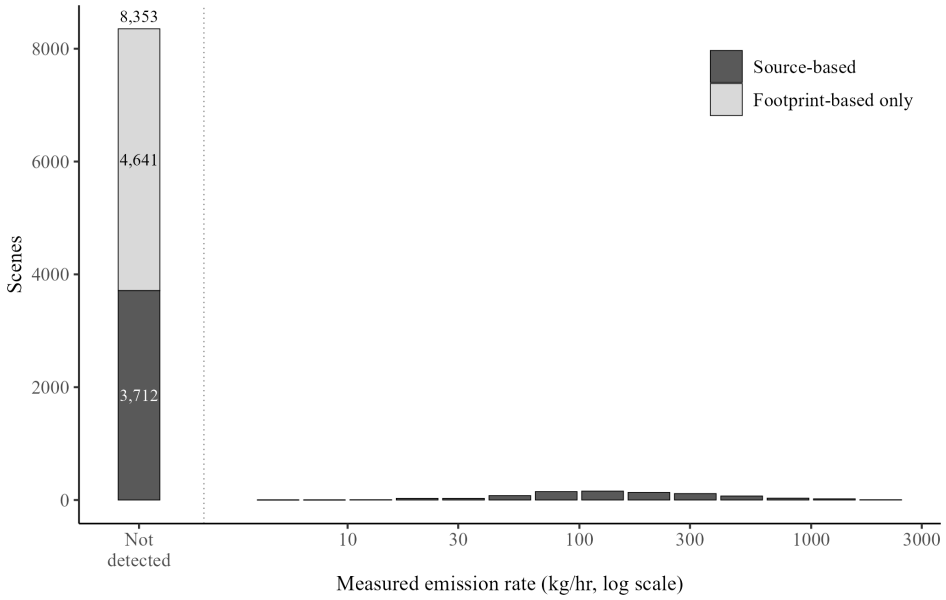


Figure 2: Distribution of measured methane emission rates at California dairies, airborne instruments only. The horizontal axis is on a log scale in kg/hr. The bar to the left of the axis break collects overpasses at which no plume was detected, split by whether the observation belongs to the source-based construction or enters only under the footprint-based construction. Overpasses at which a plume was detected but not quantified appear in neither bar.

Conditional on a quantified measurement, emission rates are large relative to the published detection limit of roughly 10 kg/hr. The 827 quantified detections average 236 kg/hr, with a median of 141 kg/hr and a standard deviation of 271 kg/hr. A further 110 overpasses record a plume that Carbon Mapper did not quantify; for those, the data establish only that emissions were above the detection limit.

How to treat the non-detects is a modeling decision with important implications for the estimation of emissions. A non-detect is not a measurement of zero. It records that the instrument resolved no distinct plume, which is consistent either with a farm that was emitting nothing or with a farm emitting at a rate the instrument could not resolve on that pass. Entering non-detects as zeros conflates the two and understates the level of emissions; assuming every zero represents a positive-emissions non-detect and entering it at the detection limit overstates the level of emissions. Section 3 treats the two conventions as bounds and reports estimates under each.

Importantly, the likelihood of non-detection seems to be correlated with observable scene characteristics such as cloud cover. This suggests that some non-detects may be due to poor observation conditions rather than the absence of emissions, reinforcing the need to carefully consider how non-detects are treated in the analysis. In Figure 3, we plot the detection probability by cloud cover for the observations in our sample. Detection probability appears to decrease as cloud cover increases, highlighting the impact of environmental conditions on the ability to detect methane emissions. That no observation has more than 50 percent is itself a reminder that aircraft fly where and when operators choose to measure, not at random.

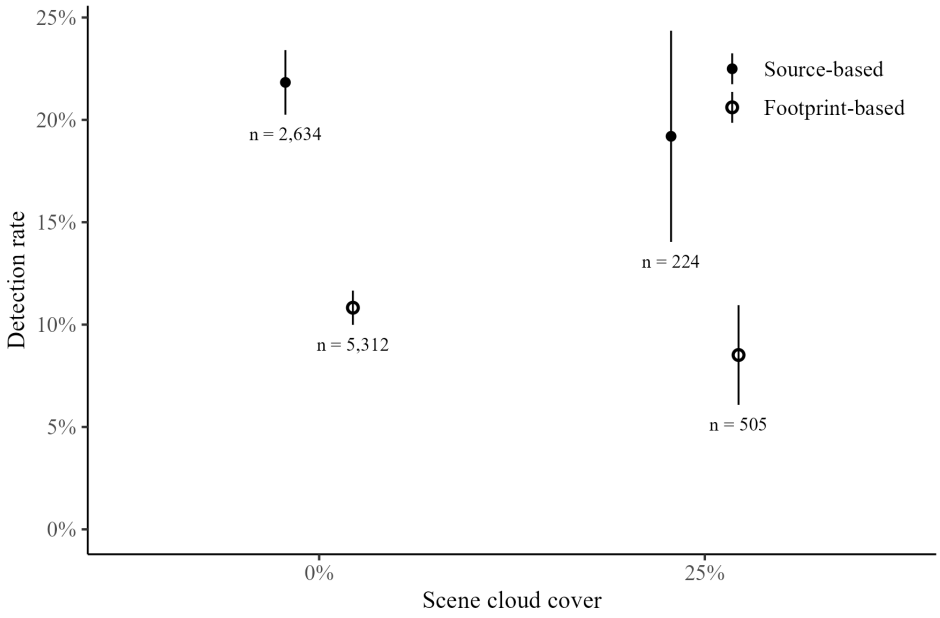


Figure 3: Detection probability by cloud cover for airborne instruments at California dairies.

5 Results

We plot the results from estimating Equation 2 with emissions and persistence on the left-hand side in Figures 4 and 5, respectively. The overall average treatment effect on emissions was estimated to be -113.22 kg/hr with a 95% confidence interval of -181.05 to -45.40 kg/hr. The overall average treatment effect on persistence was estimated to be -0.466 with a 95% confidence interval of -0.567 to -0.366. Held continuously, a reduction of 113.2 kg/hr is 992 metric tons of methane per year at a treated farm. The persistence effect is a fall of 46.6 percentage points in the share of overpasses at which a plume is detected at all, against a pre-treatment detection rate of 32.5 percent at farms that go on to adopt. Most of the emissions effect therefore operates by turning detectable plumes off rather than by shrinking them, which is what one would expect from equipment that encloses the lagoon rather than one that vents at a lower rate. [4]

Censoring A non-detect records that no plume was seen, not that the farm emitted nothing: the true emission rate lies somewhere in $[0, \text{MDL}]$. Entering every non-detect as zero therefore understates the level, and entering every non-detect at the detection limit overstates it. The two conventions bracket the truth. On the airborne sample the bracket is narrow, because a 10 kg/hr detection limit is small relative to the pre-treatment emission rate at adopting farms, which averages 78.0 kg/hr: the estimate moves from -113.22 kg/hr to -108.56 kg/hr when every non-detect is imputed at 10 kg/hr rather than zero. Both columns are reported in Table 2.

[4] We uses the airborne instruments (AVIRIS-NG, GAO, and AVIRIS-3) for our main results because their minimum detection limit is roughly 10 kg/hr (Carbon Mapper, 2026a). We exclude the spaceborne instruments, EMIT and Tanager because of their detection limits. EMIT's detection limit of roughly 250 kg/hr is higher than the median detected dairy plume of 141 kg/hr, so an EMIT look at a typical dairy could not have detected it and the zero it records is uninformative. EMIT is 67 percent of all looks at dairies and registers a detection on 0.04 percent of them. Tanager has no published detection limit; we use the 100 kg/hr as a placeholder inferred from the observed distribution, and unlike EMIT's it falls below the median detected plume. We report the corresponding estimates with the spaceborne instruments included in Appendix Section A.2.

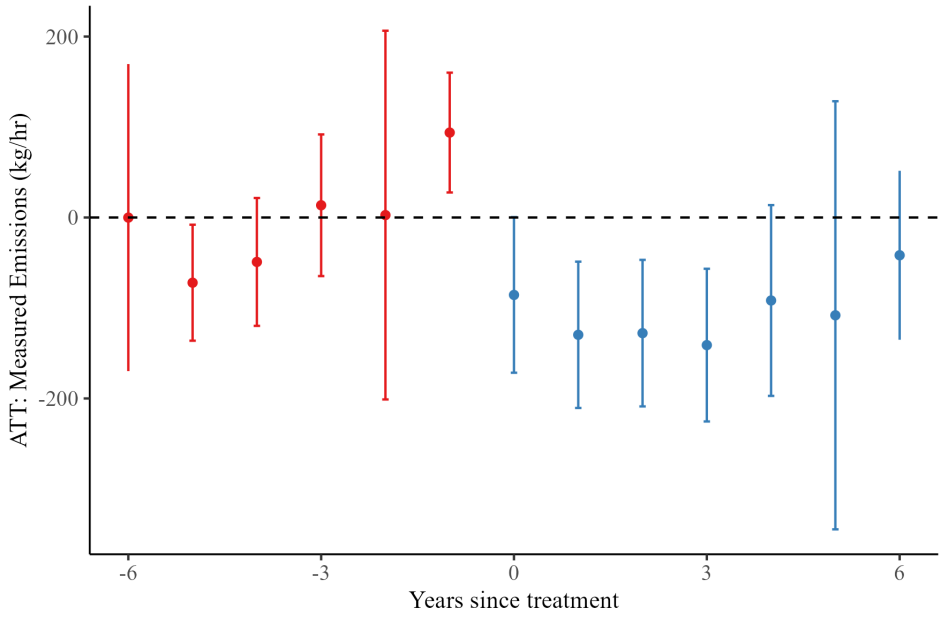


Figure 4: Estimated dynamic treatment effects of digester installation on annual mean measured emissions. Airborne instruments only; non-detects entered as zero. The x-axis indicates years relative to treatment (digester installation), with negative values representing pre-treatment years. Point estimates and 95% confidence intervals (calculated by clustering at the farm-level) are shown. The control group consists of farms not yet treated during the sample period.

Censoring at the airborne detection limit cannot account for the estimated effect. We present the point estimated average treatment effects for alternative specification in Table 2.

5.1 Comparison to TWFE

Table 3 places the Callaway–Sant'Anna estimates next to static two-way fixed-effects regressions of the same outcomes on a post-adoption indicator with farm and year fixed effects, fit to identical farm-year panels. The TWFE estimates are roughly a third the size across subsamples and both outcomes. The gap comes from the pre-treatment baseline: Callaway–Sant'Anna measures each cohort's post-treatment outcomes against its final pre-adoption year, while TWFE measures them against the farm's average over all of its pre-treatment years, and adopters' measured emissions rise ahead of adoption. The final pre-adoption year sits 54.13 kg/hr (s.e. 21.94) above the same farms' earlier pre-treatment years, within farm and net of year effects, so averaging over the pre-period pulls the baseline down and attenuates the estimate.[5] The TWFE_{-1} columns re-estimate TWFE keeping only the final pre-adoption year among treated farms' pre-treatment observations: the full-sample emissions estimate moves from -36.31 to -92.03 kg/hr, most of the way to the Callaway–Sant'Anna -113.22.

5.2 What Detection Measures

The estimates above are fit to detected emissions, so their interpretation depends on the process that generates that detection. This subsection documents properties of that process and Section

[5] Estimated on the 36 treated farms with an airborne look in their final pre-adoption year.

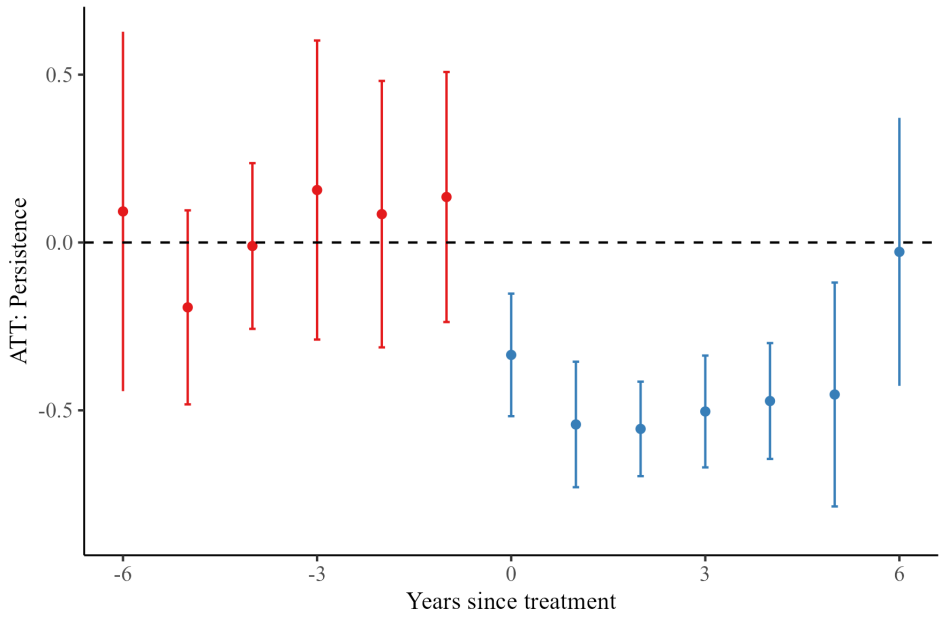


Figure 5: Estimated dynamic treatment effects of digester installation on plume persistence. Airborne instruments only. Persistence is measured as the proportion of CarbonMapper overpasses showing methane plumes. The x-axis indicates years relative to treatment (digester installation), with negative values representing pre-treatment years. Point estimates and 95% confidence intervals (calculated by clustering at the farm-level) are shown. The control group consists of farms not yet treated during the sample period.

Table 2: Estimated treatment effects for different specifications, airborne instruments only. Standard errors are given below in parentheses. "Source-based" results refer to results obtained using only observations coded as observations in the CarbonMapper Data. "Footprint-based" results refer to data constructed using the entire spatial footprint of each remote sensing observation. "Not-Yet-Treated" and "Never Treated" refer to which units are used as controls. The two emissions columns bracket the censoring: non-detects are entered as zero, which understates the emission level, or at the 10 kg/hr airborne detection limit, which overstates it.

	Measured Emissions (kg/hr)		Detection Rate
	Non-detects = 0	Non-detects = 10	(fraction)
Source-based + Not-Yet-Treated	-113.22	-108.56	-0.466
	(34.61)	(34.16)	(0.051)
Footprint-based + Not-Yet-Treated	-109.56	-105.74	-0.382
	(16.53)	(17.03)	(0.033)
Footprint-based + Never-Treated	-108.13	-104.35	-0.378
	(16.99)	(16.77)	(0.030)

Table 3: Comparison between Callaway-Sant'Anna estimates and TWFE estimates. The TWFE_{-1} column omits observations from two or more years before treatment.

	Measured Emissions (kg/hr)			Detection Rate		
	TWFE	TWFE_{-1}	CS	TWFE	TWFE_{-1}	CS
Full sample (344 farms)	-36.31	-92.03	-113.22	-0.280	-0.390	-0.466
	(12.51)	(25.43)	(34.61)	(0.039)	(0.066)	(0.051)
Ever-treated farms (94 farms)	-54.45	-47.30	-158.13	-0.343	-0.324	-0.566
	(31.37)	(49.63)	(41.77)	(0.070)	(0.089)	(0.095)
Farms $\geq$ 2,000 cows (125 farms)	-50.70	-69.95	-105.03	-0.343	-0.385	-0.483
	(18.18)	(34.57)	(21.15)	(0.054)	(0.081)	(0.077)

6.1 expands upon what those properties imply for interpreting the results.

First, detection tracks source size. Across airborne looks, the per-overpass detection rate rises monotonically from 3.6 percent at dairies under 500 cows to 27.3 percent above 4,000 (Table 4); the gradient survives instrument, year, and season fixed effects (0.081 per log cow, clustered by farm, $p < 0.001$). Detection behaves like a physical signal of source strength rather than a coin flip or strict censoring boundary. If the likelihood of detection rises with the emissions rate, then our binary detection outcome carries information about emissions.

Table 4: Per-overpass detection rate by herd size, airborne instruments (AVIRIS-NG, GAO, AVIRIS-3). "Adjusted" fixes instrument, year, and season at a common cell.

Herd size	Aircraft looks	Detected	Adjusted
<500 cows	522	3.6%	9.0%
500–1,000	894	6.2%	17.9%
1,000–2,000	1,432	7.1%	23.5%
2,000–4,000	966	20.1%	29.1%
>4,000	663	27.3%	34.7%

Second, a zero in the data doesn't necessarily mean a zero at the farm. For example, it's unlikely that dairies with more than 4,000 head of cattle have zero emissions over 70% of the time. Many of those non-detects may be emissions that were missed by the instrument rather than looks during hours when a dairy was not emitting. This is evidence that the published detection limit of 10 kg/hr for point sources likely does not carry over to emissions sources like dairies, where the emissions emanate from larger areas as opposed to a single point source. Entering non-detects as zero is therefore a lower bound on the emissions level, and we expect that entering non-detects as zeros biases our treatment effect up in magnitude. We discuss detection further in Section 6.1.

5.3 Probability of Detection

Table 5 reports estimates of Equation (8), and Figure 6 plots the fitted curve. The sample contains 305 test looks at 91 livestock sources, 174 of which detect a plume. From the 25 pairs

within an hour and the 52 pairs one to 24 hours apart in which both looks quantify a plume, the reliability of $\ln Q_r$ is 0.80 within the hour and 0.14 beyond it. A rate measured on one sortie is a weak guide to the rate on the next, and the calibration rests on few pairs.

Detection rises with the emission rate ($\hat{\beta}_Q = 0.75$, s.e. 0.38), falls with altitude ($\hat{\beta}_H = 1.07$, s.e. 0.37), and rises with distance from the swath edge ($\hat{\beta}_E = 1.38$ per km, s.e. 0.42). The wind coefficient has the expected sign but is imprecise ($\hat{\beta}_U = 0.28$, s.e. 0.17), as measurement error in ERA5 wind would predict. Figure 6 evaluates the curve at the median ERA5 wind speed among test looks, 1.7 m/s, for a source 1 km inside the swath. At the median altitude of AVIRIS-NG looks at livestock sources, 3.3 km, the emission rate detected with probability one half, Q_{50}, is 93 kg/hr (90 percent bootstrap interval 33–138). It is 113 kg/hr (57–155) at the median GAO altitude of 3.9 km and 349 kg/hr (234–1,571) at the median AVIRIS-3 altitude of 8.5 km.

The curve rises slowly in the emission rate. At $\hat{\beta}_Q = 0.75$, the rate must grow by a factor of 14 to move the detection probability from 10 to 90 percent; at the coefficient Carbon Mapper estimates for controlled point-source releases, 1.93, the factor is 2.8. We attribute the difference to the area-source problem described in Section 6.1: the same mass of methane spreads differently across lagoons, barns, and pens from one look to the next, so a given emission rate produces a detectable plume on some looks and not on others. Fitting the same model to the 190 test looks within 0.5 km of the edge gives $\hat{\beta}_Q = 0.03$ (s.e. 0.19). There, whether a plume is detected depends on where the source sits and not on how much it emits. These looks are 37 percent of airborne looks at livestock sources and 28 percent of detections, and the estimated POD does not apply to them. Appendix Figure A5 compares observed and fitted detection rates on the estimation sample.

The estimates bear on how non-detects enter the treatment-effect estimates. The Q_{50} values are about an order of magnitude above the 10 kg/hr detection limit and span the median detected airborne plume of 141 kg/hr. A non-detect is consistent with a plume well above 10 kg/hr, so entering non-detects at that limit does not bound emission levels from above; as Section 6.1 anticipates, the two imputations in Table 2 are alternative conventions rather than bounds. Using the POD to reweight the treatment-effect estimates is a work in progress. The sample consists of sources that produced at least one quantified plume, so it describes detection at sources that can be detected. Altitude and edge distance are also partly confounded: AVIRIS-3 flies higher with a wider swath and supplies nearly all test looks far from the edge. At sources that both AVIRIS-3 and GAO flew in 2024, the fitted POD predicts that AVIRIS-3 detects more often than GAO, while in the data it detects less often.

5.4 Projected versus Realized Reductions

Every digester project is written against a projected ten-year greenhouse gas reduction that the applicant reports at the time of application. The projection is the object the program pays for, and it is observable, so we can put it next to the reduction we measure from the air. Doing so requires two unit conversions and one behavioral assumption. The projections are denominated in metric tons of CO_2e, so we divide by a 100-year global warming potential of 28 to express

Table 5: Probability of detection for airborne looks at livestock sources. Maximum-likelihood estimates of Equation (8) on pairs of airborne looks at the same livestock source no more than 24 hours apart. The first column uses test looks more than 0.5 km inside the swath, the domain on which we define the POD. The second fits the same model to test looks nearer the edge and is reported as a diagnostic. Standard errors in parentheses come from 500 (first column) and 200 (second column) bootstrap samples clustered by source. Q_{50} is the emission rate detected with probability one half at the median ERA5 wind speed among test looks, 1 km inside the swath, and each instrument's median altitude; 90 percent bootstrap intervals in brackets.

	Interior looks ($e > 0.5$ km)	Near-edge looks ($e \leq 0.5$ km)
Log emission rate, β_Q	0.75	0.03
	(0.38)	(0.19)
Log ERA5 wind speed, β_U	0.28	-0.09
	(0.17)	(0.24)
Log altitude, β_H	1.07	0.63
	(0.37)	(0.34)
Distance to swath edge (km), β_E	1.38	2.11
	(0.42)	(0.70)
Constant, α	-3.61	-0.51
	(1.93)	(1.00)
Q_{50} at AVIRIS-NG altitude (3.3 km)	93 [33–138]	
Q_{50} at GAO altitude (3.9 km)	113 [57–155]	
Q_{50} at AVIRIS-3 altitude (8.5 km)	349 [234–1,571]	
Test looks	305	190
Sources	91	92
Detections	174	61
Log likelihood	-168.2	-104.9

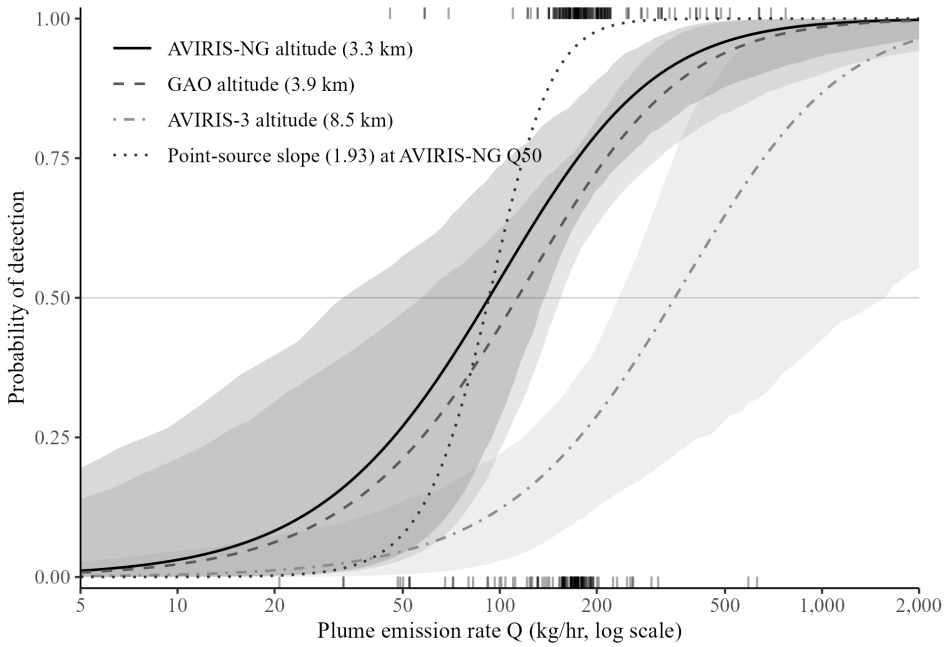


Figure 6: Fitted probability of detection for airborne looks at livestock sources. Curves evaluate Equation (8) at the estimates in Table 5, at the median ERA5 wind speed among test looks (1.7 m/s), 1 km inside the swath, and the median altitude of each instrument's looks. Shaded bands are pointwise 90 percent intervals from 500 bootstrap draws clustered by source. The dotted curve has the emission-rate coefficient of Carbon Mapper's controlled point-source releases and the same Q_{50} as the AVIRIS-NG curve. Tick marks show the calibrated reference rates of test looks that detected a plume (top) and did not (bottom).

them as tons of methane. This is the only place a GWP enters the paper.[6] We multiply our estimates in emission rates in kilograms per hour by 8,760 hours to express them as an annual flow, and by 10 to reach the projection horizon.

Table 6 reports both sides. The mean DDRDP project projects a reduction of 71.1 kg CH_4/hr and the median project 65.9 kg/hr, against a realized 113.2 kg/hr in the headline specification. The point estimate is 1.59 times the mean projection. The estimate is imprecise enough that this ordering is not established: the reduction consistent with the upper end of the confidence interval, 45.40 kg/hr, is only 0.64 times the mean projection, while the lower end is 2.55 times it. We can say that the realization rate is not obviously below one; we cannot say that digesters over-deliver against the engineering estimates.

The two sides are close enough in scale that the comparison is not driven by farm size. DDRDP projects with a reported herd size average 3,624 cows (median 3,365, $n = 102$), and the CADD digester farms adopting over our sample window average 3,157 cows. Normalizing both sides by herd size gives a projected 19.6 g CH_4/hr per cow against a realized 35.9, a ratio of 1.83 rather than 1.59.

There are three caveats worth noting for this calculation. First, there is no farm-level link between DDRDP grant projects and the farms in the estimation sample, so this pairs the average projection with the average realized reduction. It is a program-level accounting exercise so we cannot compare projected vs realized numbers at project level. Second, the estimation sample is restricted to farms an aircraft flew over and that Carbon Mapper cataloged as a source, which is not a random sample of DDRDP recipients. Third, the annualization treats an instantaneous overpass rate as an annual mean. Carbon Mapper overpasses are daytime and skew toward the warmer months, when lagoon methane production is highest, so the annualized figure is likely an upper bound on the true annual flow, and it is an upper bound on both the treated and control sides.

[6] The conversion is exact only if the projected reduction is entirely methane. If a project's reported figure also credits displaced fossil fuel or avoided grid electricity, dividing by 28 converts those CO_2 tons into methane tons that the project never promised to avert, and the projected methane reduction reported here is too large.

Table 6: Projected and realized methane reductions per farm. The DDRDP rows are the mean and median across grant projects of the applicant-reported ten-year greenhouse gas reduction, converted from MT CO_2e to tons of methane at a 100-year global warming potential of 28 and divided by the ten-year horizon. The remaining rows are the negative of the estimated overall ATT from Table 2, annualized at 8,760 hours; standard errors are in parentheses and scale linearly with the ATT standard error. All rows use airborne instruments only.

	kg CH_4/hr	t CH_4/yr
DDRDP projection (mean)	71.1	623
DDRDP projection (median)	65.9	577
Source-based + Not-Yet-Treated, non-detects = 0	113.2	992
	(34.6)	(303)
Source-based + Not-Yet-Treated, non-detects = 10	108.6	951
	(34.2)	(299)
Footprint-based + Not-Yet-Treated, non-detects = 0	109.6	960
	(16.5)	(145)
Footprint-based + Not-Yet-Treated, non-detects = 10	105.7	926
	(17.0)	(149)
Footprint-based + Never-Treated, non-detects = 0	108.1	947
	(17.0)	(149)
Footprint-based + Never-Treated, non-detects = 10	104.3	914
	(16.8)	(147)

5.5 The Cost of Abated Methane

Pairing the realized reduction with program spending gives a cost per ton of methane abated. Both cost measures are gross: the numerator is installed capital, with no revenue from gas sales, LCFS credits, or RINs netted out on either side. Across the DDRDP projects with a cost reported, mean total project cost is $5.38 million and the mean CDFA cost share is $1.61 million, so the public share averages 30 percent of project cost, below the 50 percent cap. Dividing by the realized ten-year reduction of 9,918 metric tons of methane per farm gives $162 per ton of public money and $543 per ton once the farmer's own contribution is included. The same dollars divided by the projected reduction give $258 and $860 per ton. The realized cost per ton is 0.63 times the projected cost per ton.

The social cost of a ton of methane is $2,494, and $1,778 once the CO_2 produced by burning the captured gas is netted out (U.S. Environmental Protection Agency, 2023). Public cost per realized ton is therefore 9 percent of the social cost of the methane averted, and total project cost per realized ton 31 percent. Per farm, the realized reduction is worth $17.6 million in

avoided climate damages over ten years against a mean project cost of $5.38 million.

These ratios are public dollars per realized ton conditional on the digesters that were built, which equals public dollars per ton the program caused only if no adopter would have installed without the subsidy, which we discuss in Section 6.2.

Table 7: Cost per metric ton of methane abated, in dollars, over the ten-year projection horizon, undiscounted and gross of gas and credit revenue. "Total cost" is mean installed project cost across DDRDP projects; "Public (CDFA) cost" is the mean DDRDP cost share. The DDRDP row divides those dollars by the projected reduction; the remaining rows divide the same dollars by the realized reduction implied by each specification. Standard errors, in parentheses, come from the delta method holding cost fixed. The last two rows give the social cost of a ton of methane vented and net of the CO_2 its combustion produces, for comparison.

	Total cost	Public (CDFA) cost
DDRDP projection	860	258
Source-based + Not-Yet-Treated, non-detects = 0	543	162
	(166)	(50)
Source-based + Not-Yet-Treated, non-detects = 10	566	169
	(178)	(53)
Footprint-based + Not-Yet-Treated, non-detects = 0	561	168
	(85)	(25)
Footprint-based + Not-Yet-Treated, non-detects = 10	581	174
	(94)	(28)
Footprint-based + Never-Treated, non-detects = 0	568	170
	(89)	(27)
Footprint-based + Never-Treated, non-detects = 10	589	176
	(95)	(28)
Social cost of CH_4, vented	2,494	
Social cost of CH_4, combusted to CO_2	1,778	

5.5.1 Biogas Production

Digester operators upgrade the biogas to renewable natural gas and inject it into a pipeline directly or transport it to an injection point. We approximate biogas production per cow by regressing reported biogas production in cubic feet per day on herd size through the origin, excluding projects whose reported rate equals the database default 50 cu-ft/cow/day. Accordingly, we estimate 37.9 cu-ft/cow/day (95 percent confidence interval 29.9 to 45.8, $n = 15$). At a mean digester herd of 3,157 cows and a methane share of 54.9 percent by volume, that is

23,950 mcf of salable methane per year. Figure 7 plots the AgSTAR reported biogas generation estimate against herd size for California dairy digester projects (U.S. Environmental Protection Agency, 2024).

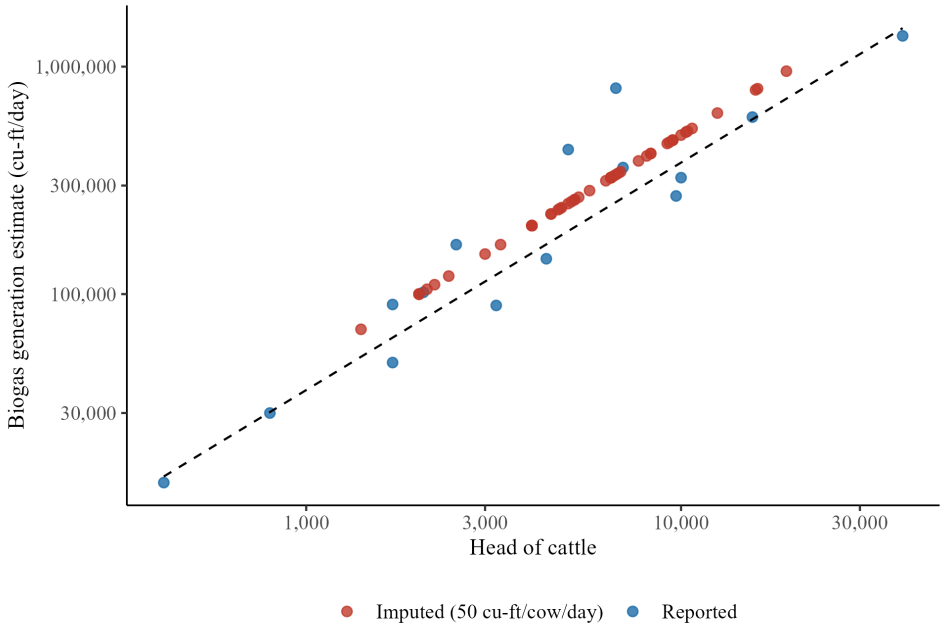


Figure 7: Biogas generation estimate against herd size, California dairy digester projects in the AgSTAR livestock anaerobic digester database. Both axes are on a log scale. Points are separated into projects reporting a rate of exactly 50 cu-ft per cow per day, which appears to be a database default rather than a measurement, and projects reporting some other rate. The dashed line is the fit through the origin on the latter group, with slope 37.9 cu-ft per cow per day.

6 Discussion

6.1 Economic Measurement and Detection Limits

Our outcome is detected emissions. Letting y_{ft} be farm f's true emission rate at overpass t and D_{ft} indicate detection, the data record $\tilde{y}_{ft} = y_{ft} \cdot D_{ft}$, with detection governed by an unknown probability-of-detection function

$$\Pr(D_{ft} = 1 \mid y_{ft}, c_{ft}, v_t) = G(y_{ft}, c_{ft}, v_t), \tag{9}$$

that depends on conditions at the farm (c: wind, cloud, surface) and characteristics of the look (v: instrument, geometry). A zero in the data conflates a farm that was not emitting with a farm the instrument missed.

A rapidly expanding literature measures economic and environmental outcomes from space, and its central methodological limitation is that remotely sensed variables are measured with error that is neither classical nor ignorable. In the most extensive characterization to date, Proctor et al. (2025) run 115 standardized experiments combining high-resolution optical imagery with

a generalizable machine-learning technology and find that it predicts roughly half the variation in ground measurements on average, with performance varying systematically across variable type, space, income, and population density—the technology supports many new measurement applications, but within quantifiable limits. In companion work, Proctor et al. (2026) show that regressions using remotely sensed variables without correction are biased in both point estimates and standard errors—more than three-quarters of conventional 95 percent confidence intervals fail to cover the true coefficient—because the measurement error is structured.

We acknowledge that treating the detection limit as a fixed number is a strong assumption. Operators of these instruments define sensitivity as a probability of detection that rises with the true emission rate, together with a limit on false positives (GHGSat, 2024). Our 10 kg/hr limit marks only one point on this curve, and the curve shifts with the conditions of each overpass. Reuland et al. (2026) show hat in their blind test, detection worked well under clear skies and low cloud cover but deteriorated above 20 percent cloud cover for every type of instrument. Clouds forced them to discard about one fifth of all responses, and detection also weakened with wind and solar angle. Our data show the same pattern. Detection probability falls as cloud cover rises, and no overpass reaches a detection probability above 50 percent. Non-detections therefore require careful treatment. Our bracket sets a non-detection to zero in one specification and to the nominal limit in the other. This bracket gives exact bounds only if detection jumps from zero to one at that limit. Under a smooth detection curve, the bracket serves as a robustness check rather than a formal bound.

We therefore estimate the probability of detection directly. We follow the functional form of Carbon Mapper's controlled-release experiments and model detection as a function of the emission rate, wind speed, aircraft altitude and the distance of the source from the edge of the scene. We identify the model from repeat looks at the same farm within 24 hours. Dunkle Werner and Qiu (2025) face a similar problem in their study of remotely sensed methane from oil and gas wells. They show that partial and targeted information about well-level emissions is still worth a great deal compared with uniform auditing. We reach a similar conclusion. An instrument that sees a farm on only a minority of overpasses can still support credible program evaluation by acknowledging the limitations of the instrument.

Airborne methane mapping was developed on oil and gas infrastructure, and a dairy is a different kind of source in ways that all suggest lower detectability. A tank vent or compressor seal releases from a compact origin and forms a coherent plume; a dairy releases from a lagoon surface of several acres and animals spread across a hundred-acre footprint, so the same mass produces a weaker, less coherent enhancement. The conventions converting enhancements to fluxes were calibrated on controlled releases dominated by oil and gas configurations; applying them to an area source is use outside the calibration set, with errors running toward missing dairy emissions. And retrieval noise in the shortwave infrared falls with surface brightness: an irrigated valley, and a dark wet lagoon in particular, sits near the worst case, exactly where the plume originates. Consistent with all of this, we detect a plume on roughly a quarter of looks even at dairies above four thousand cows.

The causal interpretation of our results rests on a few identifying assumptions beyond the

standard difference-in-differences conditions of Section 3. The first is an exclusion restriction. We assume that the detection function is invariant to treatment except through emissions (this assumption is potentially at risk because a covered lagoon converts a diffuse source into a structure with discrete vents, plausibly more detectable per unit methane—which would make our persistence estimate conservative—and Valdez et al. (2026) report exactly that shift in post-installation plume sources). Second, that observing conditions are independent of treatment given controls (plausible given that the conditions of aircraft flights seem balanced over time). Third, that parallel trends holds in the latent emission rate rather than the detection indicator. Fourth, that the estimand is point-source manure methane, the component a digester targets, not whole-farm methane including enteric emissions (Beauchemin et al., 2025). Lastly, we assume that plume attribution between neighboring farms is stable.

We plot the per-overpass detection rate against herd size for farms that never adopt, for adopters before installation and for adopters after installation in Figure 8. The two untreated series provide a check on selection. If adopters and never-adopters of the same herd size emit similar amounts and are observed under similar conditions, the two series should coincide. The post-installation series then carries information about the treatment effect. If emissions scale with herd size and the digester reduces them by a constant factor, the post-installation curve is a horizontal shift of the pre-installation curve on a logarithmic herd-size axis, and the size of this shift measures the proportional reduction in emissions. This comparison does not require knowing the detection function, provided the distribution of overpass conditions is the same across groups. Combined with the estimated probability of detection from Section 3.4, it also yields the reduction in kilograms per hour and allows for differences in conditions between groups. Non-detections therefore remain informative about treatment effects when the instrument's probability of detection is known or estimated.

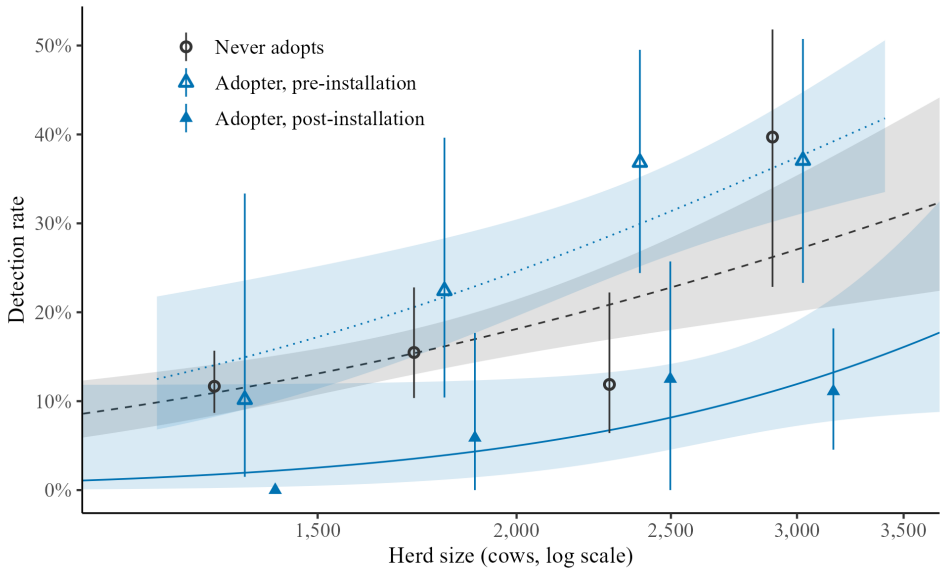


Figure 8: Per-overpass detection rate against herd size for farms that never adopt a digester, adopters observed before installation, and adopters observed after.

6.2 Additionality

We assume that adopters would not have installed the digester without the cost share program, based on findings of a nationwide digester operator survey. These results suggest that 70 percent of operators rated cost share programs important or very important for their existing digester, and 79 percent report they would not have built the digester without cost share support. Among surveyed California digester operators, only one reported that cost share programs were "very unimportant" to their current digester, and none rated such programs as unimportant for prospective digesters, with responses ranging from neutral to very important. This suggests that the share of digesters that would have been constructed without cost share support is likely negligible. The self reported average cost share received was 57 percent of total project cost (Wehner et al., 2026).

We nonetheless report the cost per ton under two additionality scenarios. If every subsidized digester is additional, the causal cost per ton equals the accounting cost and we calculate $162 per ton of methane in public funds and $543 per ton in total installed cost in Table 7. If instead only the survey-implied share $s = 0.79$ of adopters is additional, the program's dollars purchase abatement only at additional farms, and the cost per caused ton scales by $1/s$: $205 public and $687 total. Both scenarios leave the public cost per caused ton at nine or twelve percent of the $1,778 social cost per combusted ton. That comparison counts only the DDRDP cost share and omits LCFS credits and RINs currently, the ratio should be therefore interpreted as a lower bound.

7 Conclusion

We measure whether subsidized anaerobic digesters reduce measured methane emissions, and whether realized reductions match the projections the subsidies were based on. Matching aerial point-source retrievals to 2,115 California dairies and the administrative records of the state's digester cost-share program, and comparing adopting farms to farms whose installation has not yet occurred, we find that digester installation reduces measured emissions by 113 kg CH_4/hr—roughly 992 tons of methane per farm-year—and cuts the share of overpasses with a detectable plume by 47 percentage points. The realized reduction is 1.59 times the mean engineering projection, though the confidence interval does not rule out under-delivery; the public cost per realized ton, $162 undiscounted, is 9 percent of the social cost of the methane averted; and 79 percent of surveyed operators report they would not have installed without cost share.

Our results are subject to the following limitations. The outcome is detected emissions, and a non-detect cannot distinguish a farm that was not emitting from one the instrument missed, so the persistence effect measures movement out of the detectable class instead of a percentage reduction. The estimated reduction exceeds the mean pre-treatment emission rate at adopters, so part of the effect reflects rising counterfactual emissions at not-yet-treated farms. The estimation sample is limited to farms that aircraft overflew, which is not necessarily random.

The findings demonstrate how agri-environmental programs can be evaluated and that they are an effective tool in contributing to emission reduction targets (United Nations Environment

Programme, 2026). These results call for further evaluations of agri-environmental payments, for example, enteric methane feed additives in dairy or digester programs in other states. Our results demonstrate that advancements in emission measurements can be combined with the use of administrative data, an example that could contribute to climate accountability as emissions measurement technology scales.

References

Ai, Jianwei, Qinan Lu, and Wendong Zhang, "Measuring Livestock from Space: Global and U.S. Evidence on the Detection, Attribution, and Limits of Satellite Methane," 2026. Working paper.

Aker, Jenny C., Jennifer Burney, Alison Campion, B. Kelsey Jack, and Chuan Liao, "How Many (Half) Moons? Measuring Technology Adoption from the Sky and on the Ground," *AEA Papers and Proceedings*, May 2026, *116*, 173–177.

Arndt, C., A.B. Leytem, A.N. Hristov, D. Zavala-Araiza, J.P. Cativiela, S. Conley, C. Daube, I. Faloona, and S.C. Herndon, "Short-term Methane Emissions from 2 Dairy Farms in California Estimated by Different Measurement Techniques and US Environmental Protection Agency Inventory Methodology: A Case Study," *Journal of Dairy Science*, December 2018, *101* (12), 11461–11479.

Baker, Andrew, Brantly Callaway, Scott Cunningham, Andrew Goodman-Bacon, and Pedro H. C. Sant'Anna, "Difference-in-Differences Designs: A Practitioner's Guide," *Journal of Economic Literature*, June 2026, *64* (2), 498–557.

Baldé, Hambaliou, Claudia Wagner-Riddle, Douglas MacDonald, and Andrew VanderZaag, "Fugitive Methane Emissions from Two Agricultural Biogas Plants," *Waste Management*, September 2022, *151*, 123–130.

Beauchemin, Karen A., Ermias Kebreab, Michelle Cain, and Michael J. VandeHaar, "The Path to Net-Zero in Dairy Production: Are Pronounced Decreases in Enteric Methane Achievable?," *Annual Review of Animal Biosciences*, 2025, *13*, 325–341.

Borusyak, Kirill, Xavier Jaravel, and Jann Spiess, "Revisiting Event-Study Designs: Robust and Efficient Estimation," *The Review of Economic Studies*, 2024, *91* (6), 3253–3285.

Burlig, Fiona, Christopher Knittel, David Rapson, Mar Reguant, and Catherine Wolfram, "Machine Learning from Schools about Energy Efficiency," *Journal of the Association of Environmental and Resource Economists*, 2020, *7* (6), 1181–1217.

Butters, R. Andrew, Jackson Dorsey, and Ivan Rudik, "Pollution Pricing in Equilibrium: Production, Reallocation, and Aggregate Impacts," Working Paper 35682, National Bureau of Economic Research August 2026.

Calbry-Muzyka, Adelaide, Hossein Madi, Florian Rüsch-Pfund, Marta Gandiglio, and Serge Biollaz, "Biogas Composition from Agricultural Sources and Organic Fraction of Municipal Solid Waste," *Renewable Energy*, 2022, *181*, 1000–1007.

California Air Resources Board, "Public Hearing to Consider Amendments to the Low Carbon Fuel Standard: Final Statement of Reasons, Appendix B—Summary of Comments and Agency Response," Technical Report, California Air Resources Board 2024.

_ , "Low Carbon Fuel Standard Regulation," Technical Report, California Air Resources Board 2025. Final Regulation Order approved by the Office of Administrative Law June 27, 2025; effective July 1, 2025. Unofficial electronic version.

California Department of Food and Agriculture, "CDFA Dairy Digester Research and Development Program Funded Projects Report," Program Report 2025. Report to the California Legislature.

_ , "Alternative Manure Management Program (AMMP)," https://www.cdfa.ca.gov/oars/ammp/ 2026. Office of Agricultural Resilience and Sustainability. Accessed August 6, 2026.

California Public Utilities Commission, "Bioenergy Feed-in Tariff Program (SB 1122)," https://www.cpuc.ca.gov/industries-and-topics/electrical-energy/electric-power-procurement/rps/rps-procurement-programs/rps-sb-1122-biomat 2026. Accessed August 6, 2026.

California State Legislature, "Senate Bill No. 1383: Short-lived Climate Pollutants: Methane Emissions: Dairy and Livestock: Organic waste: Landfills," https://leginfo.legislature.ca.gov/faces/billTextClient.xhtml?bill_id=201520160SB1383 2016. Chapter 395, approved by Governor September 19, 2016.

_ , "SB 919: Biomethane Monetary Incentive Program," https://calmatters.digitaldemocracy.org/bills/ca_202520260sb919 2026. 2025–2026 Regular Session, Senate. Amended in Senate April 28, 2026.

Callaway, Brantly and Pedro H. C. Sant'Anna, "Difference-in-Differences with Multiple Time Periods," *Journal of Econometrics*, 2021, *225* (2), 200–230.

Carbon Mapper, "Frequently Asked Questions," 2026. Accessed: 2026-08-18.

_ , "Methane Emissions Data from the Carbon Mapper Data Portal," Open data from the Carbon Mapper public data portal 2026. Accessed on 12 January 2026.

Chen, Chen-Ti, Gabriel E. Lade, John M. Crespi, and David A. Keiser, "Size-based Regulation and Water Quality: Evidence from the Iowa Hog Industry," *American Journal of Agricultural Economics*, 2025, *108* (3), 829–855.

Christensen, Peter, Paul Francisco, Erica Myers, and Mateus Souza, "Decomposing the Wedge between Projected and Realized Returns in Energy Efficiency Programs," *The Review of Economics and Statistics*, 2023, *105* (4), 798–817.

de Chaisemartin, Clément and Xavier D'Haultfœuille, "Two-Way Fixed Effects Estimators with Heterogeneous Treatment Effects," *American Economic Review*, 2020, *110* (9), 2964–2996.

Debruyn, Zachary, Andrew VanderZaag, and Claudia Wagner-Riddle, "Increased Dairy Farm Methane Concentrations Linked to Anaerobic Digester in a Five-Year Study," *Journal of Environmental Quality*, March 2020, *49* (2), 509–515.

Forster, Piers, Trude Storelvmo, Kyle Armour, William Collins, Jean-Louis Dufresne, David Frame, Daniel J. Lunt, Thorsten Mauritsen, Matthew D. Palmer, Masahiro Watanabe, Martin Wild, and Hua Zhang, "The Earth's Energy Budget, Climate Feedbacks, and Climate Sensitivity," in V. Masson-Delmotte, P. Zhai, A. Pirani et al., eds., *Climate Change 2021: The Physical Science Basis. Contribution of Working Group I to the Sixth Assessment Report of the Intergovernmental Panel on Climate Change*, Cambridge, United Kingdom and New York, NY, USA: Cambridge University Press, 2021, pp. 923–1054.

Fowlie, Meredith, Michael Greenstone, and Catherine Wolfram, "Do Energy Efficiency Investments Deliver? Evidence from the Weatherization Assistance Program," *The Quarterly Journal of Economics*, 2018, *133* (3), 1597–1644.

Friends of the Earth, "Environmental, Agriculture, and Community Groups Applaud Extended Pause of Manure Digester Federal Funding," https://foe.org/news/extended-pause-of-manure-digester-federal-funding/ April 2026. Press release. Accessed August 6, 2026.

GHGSat, "Validation and Metrics for Emissions Detection by Satellite," https://www.ghgsat.com/resources/validation-and-metrics-for-emissions-detection-by-satellite/ 2024. Accessed August 11, 2026.

Goodman-Bacon, Andrew, "Difference-in-Differences with Variation in Treatment Timing," *Journal of Econometrics*, 2021, *225* (2), 254–277.

Henningsen, Arne, Guy Low, David Wuepper, Tobias Dalhaus, Hugo Storm, Dagim Belay, and Stefan Hirsch, "Estimating Causal Effects With Observational Data: Guidelines for Agricultural and Applied Economists," *Journal of Agricultural Economics*, December 2025.

Hersbach, Hans, Bill Bell, Paul Berrisford, Shoji Hirahara, András Horányi, Joaquín Muñoz-Sabater, Julien Nicolas, Carole Peubey, Raluca Radu, Dinand Schepers et al., "The ERA5 Global Reanalysis," *Quarterly Journal of the Royal Meteorological Society*, 2020, *146* (730), 1999–2049.

Intergovernmental Panel on Climate Change (IPCC), "Chapter 10: Emissions from Livestock and Manure Management," in "2019 Refinement to the 2006 IPCC Guidelines for National Greenhouse Gas Inventories, Volume 4: Agriculture, Forestry and Other Land Use," Intergovernmental Panel on Climate Change, 2019.

Lazenby, Ruthie, "Mitigating Emissions From California Dairies," Emmett Institute on Climate Change and the Environment. Link January 2024.

Magesh, Varun, Claire Morton, Qinfan Lyu, Jamie Harding, Frank C. Curriero, Cara Wychgram, Sara Lupolt, Keeve Nachman, Elena Eneva, and Daniel E.

Ho, "Do Methane Mitigation Incentives Intensify Livestock Production? Evidence from California, 2016-2025," *Unpublished*, 2025.

Proctor, Jonathan, Tamma Carleton, and Sandy Sum, "Parameter Recovery Using Remotely Sensed Variables," *Journal of the Association of Environmental and Resource Economists*, 2026. forthcoming.

_ , _ , Trinetta Chong, Taryn Fransen, Simon Greenhill, Jessica Katz, Hikari Murayama, Luke Sherman, Jeanette Tseng, Hannah Druckenmiller, and Solomon Hsiang, "What Can Satellite Imagery and Machine Learning Measure?," Working Paper 34315, National Bureau of Economic Research 2025.

Reuland, Frances E., Taylor Adams, Evan D. Sherwin, Sahar H. El Abbadi, Eric A. Kort, and Adam R. Brandt, "Evaluating Space-Based Methane Detection Through a One-Year Blind Test," *Nature*, 2026, *658*, 673–681.

Rodriguez, Michael V., Nidia Rojas Robles, Valerie Carranza, Ranga Thiruvenkatachari, Mariana Reyes, Chelsea V. Preble, Joyce Pexton, Deanne Meyer, Ray G. Anderson, Akula Venkatram, and Francesca M. Hopkins, "Anaerobic Digester Installation Significantly Reduces Liquid Manure Management CH_4 Emissions at a California Dairy Farm," *GCB Bioenergy*, June 2025, *17* (7).

Rossi, Gemma Del, Mohammad Mainul Hoque, Yongjie Ji, and Catherine L. Kling, "The Economics of Nutrient Pollution from Agriculture," *Annual Review of Resource Economics*, October 2023, *15* (1), 105–130.

Roth, Jonathan, "Pretest with Caution: Event-Study Estimates after Testing for Parallel Trends," *American Economic Review: Insights*, 2022, *4* (3), 305–322.

_ and Pedro H. C. Sant'Anna, "When Is Parallel Trends Sensitive to Functional Form?," *Econometrica*, 2023, *91* (2), 737–747.

_ , _ , Alyssa Bilinski, and John Poe, "What's Trending in Difference-in-Differences? A Synthesis of the Recent Econometrics Literature," *Journal of Econometrics*, 2023, *235* (2), 2218–2244.

Sant'Anna, Pedro H. C. and Jun Zhao, "Doubly Robust Difference-in-Differences Estimators," *Journal of Econometrics*, 2020, *219* (1), 101–122.

Seber, Gonca, Nikita Pavlenko, and Chelsea Baldino, "Evaluating the policy value of dairy biomethane-derived hydrogen in California's Low Carbon Fuel Standard," Technical Report, International Council on Clean Transportation September 2024.

Sun, Liyang and Sarah Abraham, "Estimating Dynamic Treatment Effects in Event Studies with Heterogeneous Treatment Effects," *Journal of Econometrics*, 2021, *225* (2), 175–199.

United Nations Environment Programme, "Emissions Gap Report 2026: The Point of Return," Technical Report, United Nations Environment Programme, Nairobi 2026.

U.S. Environmental Protection Agency, "Market Opportunities for Biogas Recovery Systems at U.S. Livestock Facilities," Technical Report EPA-430-R-18-006, AgSTAR Program, Washington, DC 2018.

_ , "EPA Report on the Social Cost of Greenhouse Gases: Estimates Incorporating Recent Scientific Advances," 2023.

_ , "Livestock Anaerobic Digester Database," Accessed July 2024 June 2024. Data compiled from information available through June 2024.

_ , "Methane Emissions," United States Environmental Protection Agency Link January 2026.

Valdez, Alyssa, Riley Duren, Daniel H Cusworth, Nidia E Rojas-Robles, Diana Rodriguez Amezquita, and Francesca M Hopkins, "Evaluating the impact of anaerobic digesters on point source methane emissions from California dairies from remote sensing," *Environmental Research Letters*, March 2026.

Wehner, Jasmin, Wendong Zhang, Christopher A. Wolf, Lauren Ray, and David McLaughlin, "Drivers of Current and Future Anaerobic Digester Investment on U.S. Dairy Farms," *JDS Communications*, 2026.

Werner, Karl Dunkle and Wenfeng Qiu, "Information Matters: Feasible Policies for Reducing Methane Emissions," *Journal of the Association of Environmental and Resource Economists*, 2025, *12* (5), 1389–1429.

Wooldridge, Jeffrey M., "Two-Way Fixed Effects, the Two-Way Mundlak Regression, and Difference-in-Differences Estimators," *Empirical Economics*, 2025, *69*, 2545–2587.

Wuepper, David, Wyclife Agumba Oluoch, and Hadi Hadi, "Satellite Data in Agricultural and Environmental Economics: Theory and Practice," *Agricultural Economics*, March 2025, *56* (3), 493–511.

A Appendix

A.1 Additional Details On Carbon Mapper Detections

Using the Footprint-Based Observation Set Our primary results use only farms that were coded as being "observed" by Carbon Mapper. However, Carbon Mapper provides geospatial footprints of the swath of each observation. Therefore, there are many "observations" which are not included in the main specifications. First, some farms are never observed emitting, so they are never included in the list of Carbon Mapper sources. Second, Carbon Mapper appears to only code a source as being "observed" if it was observed under favorable conditions. In these results, we spatially merge the footprint of each observation with our universe of farms, and include the many implicit zeros (from observations that were presumably observed but not coded as being observed).

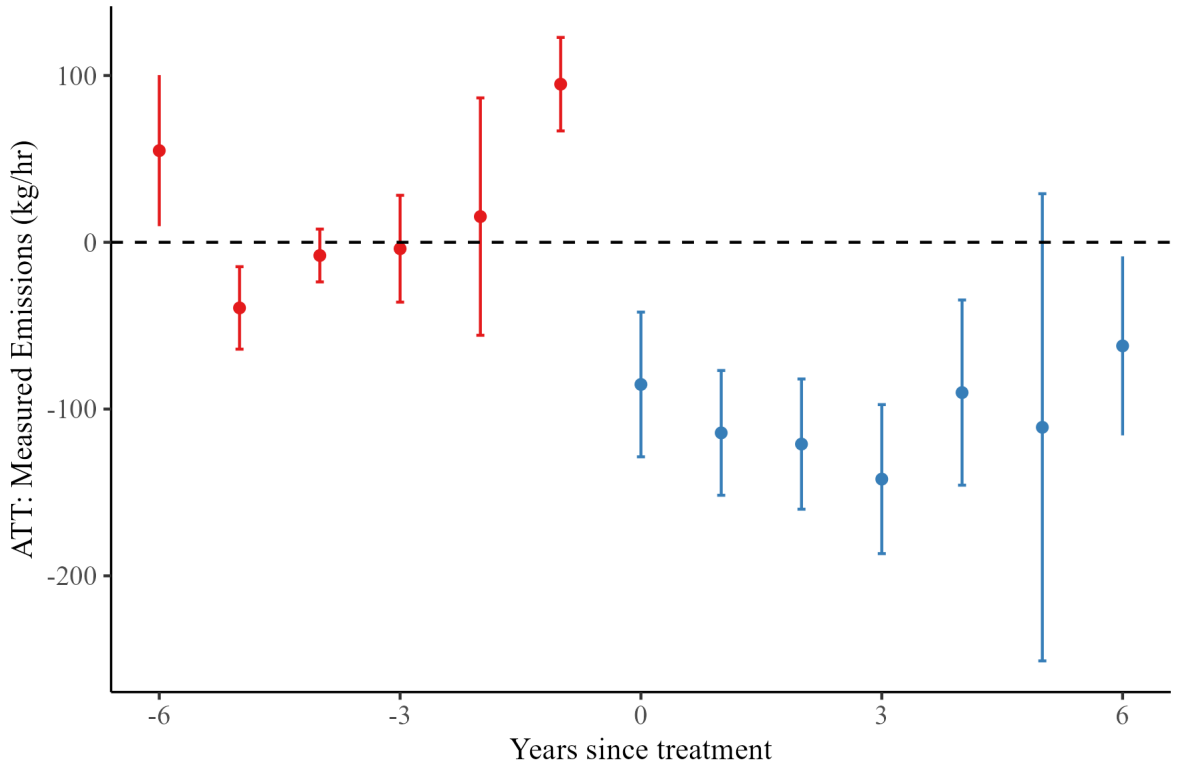


Figure A1: Estimated dynamic treatment effects on mean measured emissions, using the footprint-based observation set. Airborne instruments only; non-detects entered as zero.

A.2 Carbon Mapper: Including the Spaceborne Instruments

The main specifications use only the airborne instruments. Here we add the two spaceborne instruments, EMIT and Tanager. Doing so adds 33 detections, taking the count from 937 to 970, while adding far more looks than detections. How many more depends on the construction. In the source-based observation set the spaceborne instruments barely move the look count, from 4,649 to 4,717, because a look enters that set only when Carbon Mapper certifies it as an observation of a catalogued source. In the footprint-based set, where every scene covering a farm

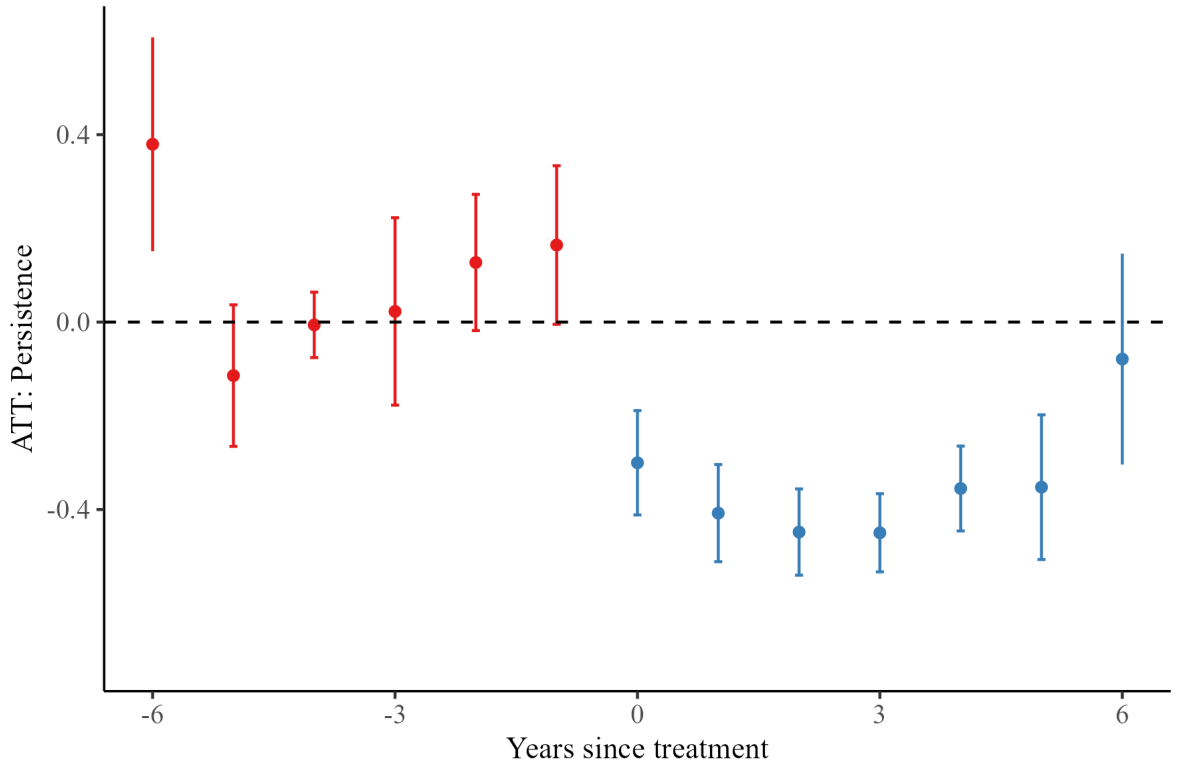


Figure A2: Estimated dynamic treatment effects on plume persistence, using the footprint-based observation set. Airborne instruments only.

counts, they multiply looks by a factor of 3.7, from 9,290 to 34,665. Either way the additional observations are overwhelmingly zeros, because EMIT's detection limit of roughly 250 kg/hr exceeds the median detected dairy plume of 148.3 kg/hr and EMIT records a detection on 0.04% of its looks at dairies. Those zeros are looks that could not have detected a typical dairy, rather than evidence that the farm was not emitting.

The point estimates are close to the main specification, as Table A1 shows. What the spaceborne instruments change is not the answer but the range of emission levels consistent with the data. We report only the convention that enters non-detects as zero. The airborne bracket in Table 2 has no counterpart here: imputing a spaceborne non-detect at its own detection limit would assign the farm an emission rate above that of a typical dairy, which the data cannot support.

A.3 Probability of Detection: Fit Check

Figure A5 compares observed and fitted detection rates for the probability-of-detection model in Section 5.3.

B Treatment Effects With Imperfect Detection

This appendix shows that if the detection function G in Equation (9) were known, the treatment effect on latent emissions would be point-identified with no model of the emission distribution.

Table A1: Estimated treatment effects including the spaceborne instruments (EMIT and Tanager) alongside the airborne ones. Standard errors are given below in parentheses. Non-detects are entered as zero. Columns and rows are otherwise defined as in Table 2.

	Measured Emissions (kg/hr)	Detection Rate (fraction)
Source-based + Not-Yet-Treated	-122.66	-0.398
	(37.86)	(0.073)
Footprint-based + Not-Yet-Treated	-101.70	-0.315
	(17.19)	(0.034)
Footprint-based + Never-Treated	-100.63	-0.313
	(16.08)	(0.030)

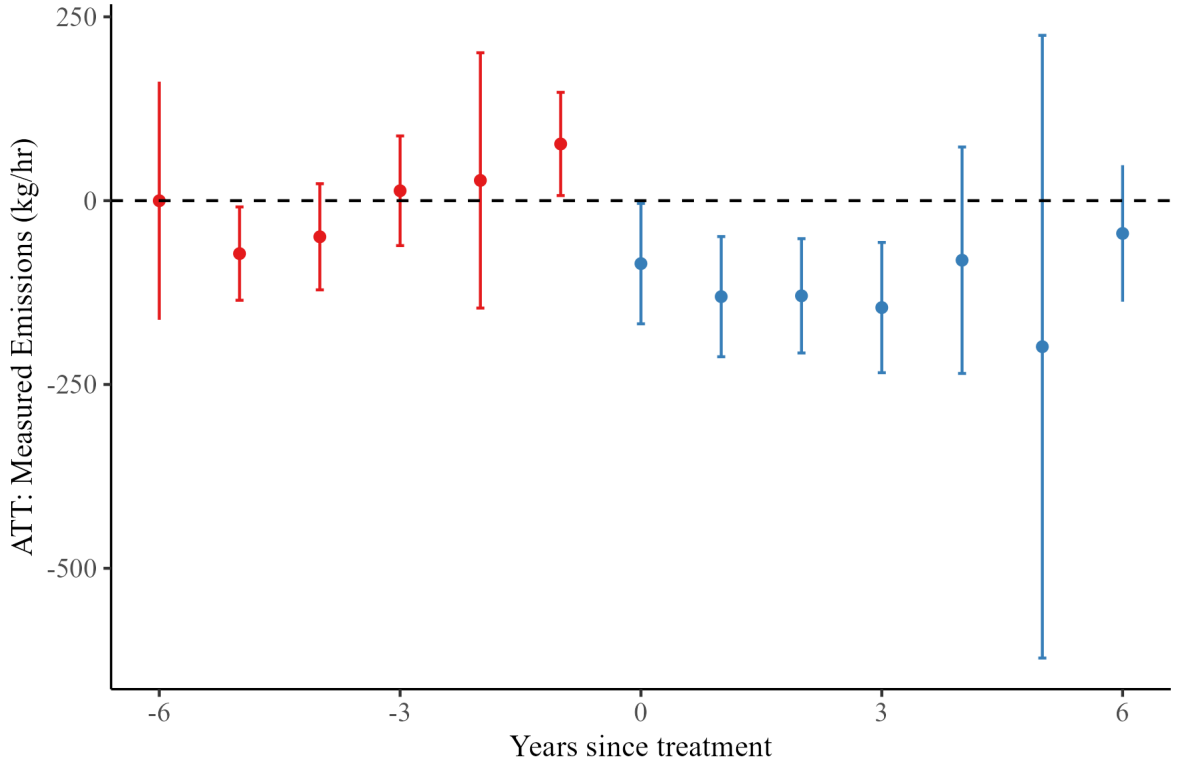


Figure A3: Estimated dynamic treatment effects on mean measured emissions, including the satellite instruments. Source-based observations; non-detects entered as zero.

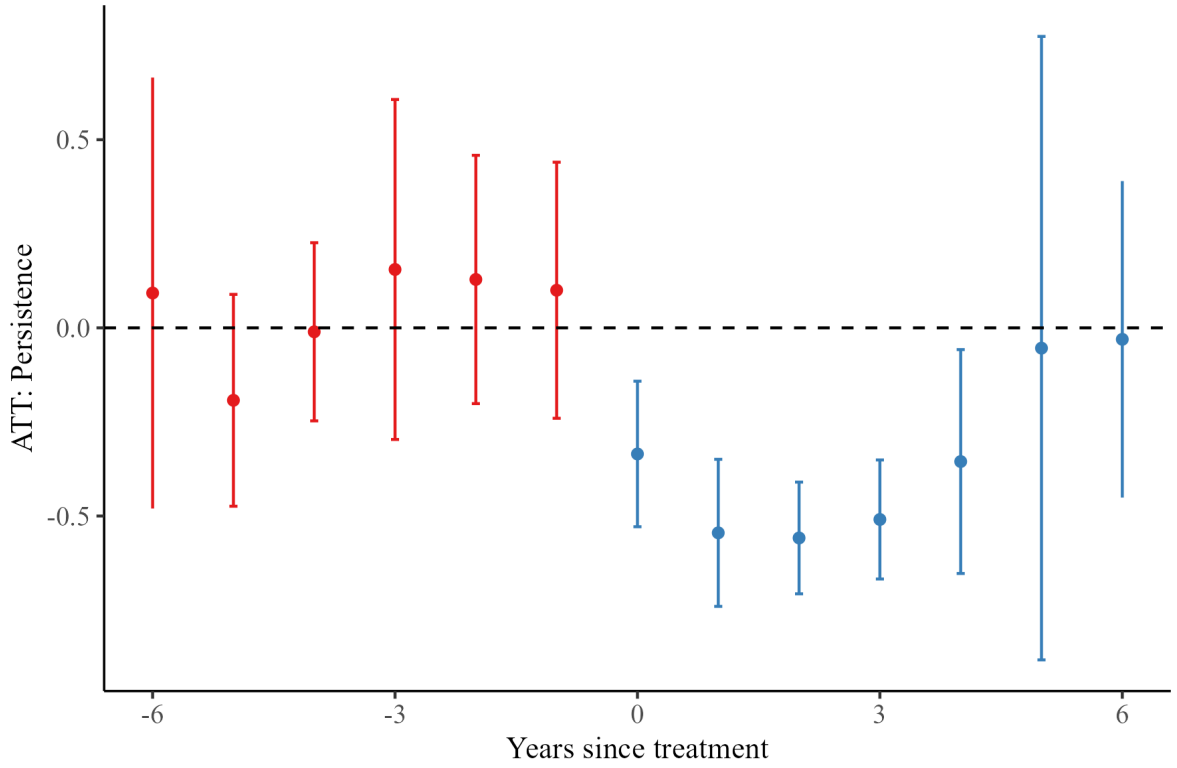


Figure A4: Estimated dynamic treatment effects on plume persistence, including the satellite instruments. Source-based observations.

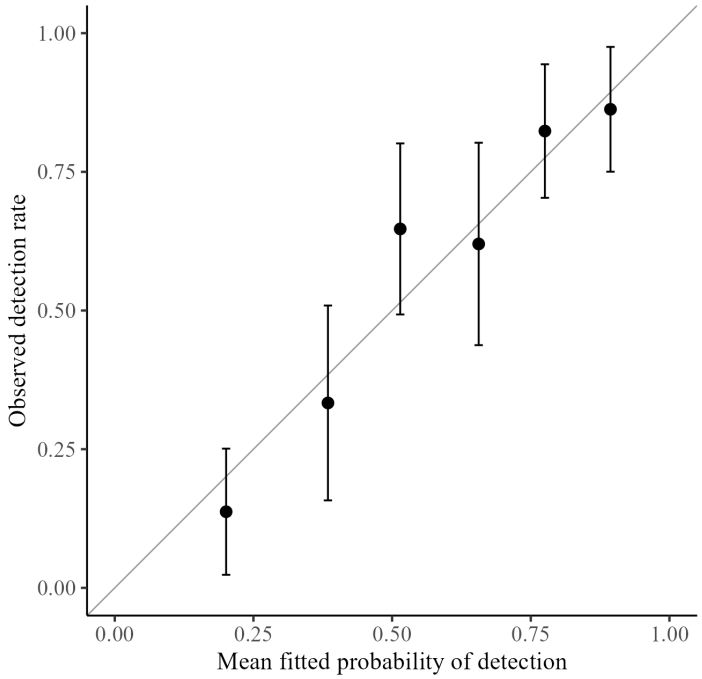


Figure A5: Observed and fitted detection rates for the probability-of-detection model. Test looks are grouped into sextiles of fitted probability. Each point plots the observed detection rate against the mean fitted probability, with a 95 percent interval clustered by source. The line is the 45-degree line.

Let $T_{ft} \in \{0, 1\}$ denote digester status at the time of look t, and let f_T be the density of the latent emission rate y_{ft} among looks with $T_{ft} = T$. Assume $G(u) > 0$ for every positive emission rate: detection can be arbitrarily unlikely, but never impossible. Conditioning on the look conditions c_{ft} and v_t is suppressed throughout; every statement holds at fixed conditions.[7]

Among looks at group-T farms emitting at rate u, a fraction $G(u)$ are detected. The detected sample therefore over-represents high emitters, but it does so in a way we know exactly: the density of measured values among detected looks is the latent density tilted by G,

$$\tilde{f}_T(u) = \frac{G(u)\, f_T(u)}{p_T}, \qquad p_T \equiv \Pr(D_{ft} = 1 \mid T) = \int G(u)\, f_T(u)\, du, \tag{10}$$

where dividing by the group's detection rate p_T makes the tilted density integrate to one. Everything in Equation (10) except f_T is known or observable: G is known by assumption, p_T is the observed detection rate, and $\tilde{f}_T$ is the observed distribution of detected values. Solving for the one unknown,

$$f_T(u) = p_T \cdot \frac{\tilde{f}_T(u)}{G(u)}. \tag{11}$$

In words, to undo the over-representation, weight each detected value by $1/G(u)$: a plume measured at a rate the instrument catches one time in ten stands in for ten looks at farms emitting at that rate, nine of which were recorded as zeros. The weight is computable because on detected looks $\tilde{y}_{ft} = y_{ft}$, so the true rate is observed exactly where G must be evaluated. And because $G > 0$ everywhere, no part of the distribution is skipped: the right-hand side of Equation (11) integrates to one, so the whole latent density is identified, not only its mean. The mean follows by integrating,

$$\mathbb{E}[y \mid T] = \int u\, f_T(u)\, du = p_T \cdot \mathbb{E}\left[\frac{\tilde{y}_{ft}}{G(\tilde{y}_{ft})} \;\middle|\; D_{ft} = 1,\, T\right]. \tag{12}$$

As a recipe: within a digester group, divide each detected value by its own detection probability, average those ratios, and multiply by the group's detection rate. Doing this for each group and differencing point-identifies $\Delta \equiv \mathbb{E}[y \mid T = 1] - \mathbb{E}[y \mid T = 0]$, with f_T left completely free.

A numerical example fixes ideas. Suppose half of a group's farm-hours emit 100 kg/hr and half emit 400, and suppose $G(100) = 0.1$ and $G(400) = 0.5$. The true mean is 250. The detection rate is $p = 0.5(0.1) + 0.5(0.5) = 0.3$, and among detections one sixth are 100s and five sixths are 400s. The raw detected average is $\frac{1}{6}(100) + \frac{5}{6}(400) = 350$, too high because the 400s are five times easier to see. Reweighting by Equation (12) gives $0.3 \times \left[\frac{1}{6}\frac{100}{0.1} + \frac{5}{6}\frac{400}{0.5}\right] = 250$, exactly the truth. For comparison, the zeros-imputed mean, averaging $\tilde{y}$ over all looks with non-detects counted as zero, is $0.5(0.1)(100) + 0.5(0.5)(400) = 105$, less than half the truth. That object, $\int u\, G(u)\, f_T(u)\, du$, is what the zeros specification in Section 5 estimates, and it understates the level wherever $G < 1$.

[7] The derivation treats every detection as quantified. In practice some detected plumes are unquantified; those looks would need the same right-censored treatment they receive in the main specifications.